Article

Current Biology

A thalamo-preoptic pathway promotes social grooming in rodents

Graphical abstract

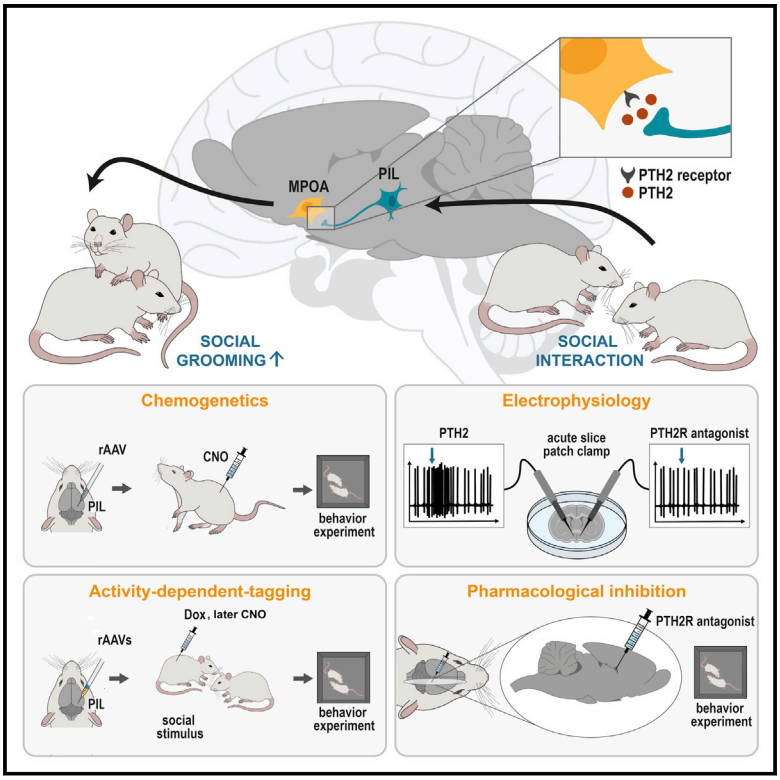

Highlights

- Social interaction increases activity in the posterior thalamus (PIL)
- The activity of socially tagged PIL neurons drives social grooming behavior
- PTH2-neuropeptide-expressing PIL neurons project to the preoptic area (MPOA)
- The PTH2 neurons excite MPOA cells and in turn control social grooming

Authors

Dávid Keller, Tamás Láng, Melinda Cservenák, ..., Mazahir T. Hasan, Valery Grinevich, Arpád Dobolyi

Correspondence

valery.grinevich@zi-mannheim.de (V.G.), dobolyi.arpad@ttk.elte.hu (A.D.)

In brief

Social grooming is important for both individuals and to establish social communities. Keller et al. discover a thalamo-hypothalamic PIL-MPOA pathway critical for grooming between rodents and also demonstrate a similar pathway in the human brain. The pathway bypasses the cerebral cortex and thus might independently transmit unconscious pleasure.

Keller et al., 2022, Current Biology *32*, 1–14
November 7, 2022
https://doi.org/10.1016/j.cub.2022.08.062

CellPress

Please cite this article in press as: Keller et al., A thalamo-preoptic pathway promotes social grooming in rodents, Current Biology (2022), https://doi.org/10.1016/j.cub.2022.08.062

Current Biology

CellPress

Article

A thalamo-preoptic pathway promotes social grooming in rodents

Dávid Keller,[1,2] Tamás Láng,[1] Melinda Cservenák,[2] Gina Puska,[2,3] János Barna,[1] Veronika Csillag,[4,5] Imre Farkas,[4,6] Dóra Zelena,[7,8] Fanni Dóra,[1,2,9] Stephanie Küppers,[10] Lara Barteczko,[10] Ted B. Usdin,[11] Miklós Palkovits,[9] Mazahir T. Hasan,[12,13] Valery Grinevich,[10,*] and Arpád Dobolyi[2,14,*]

[1]Laboratory of Neuromorphology, Department of Anatomy, Histology and Embryology, Semmelweis University, Budapest 1094, Hungary
[2]ELKH-ELTE Laboratory of Molecular and Systems Neurobiology, Department of Physiology and Neurobiology, Eötvös Loránd Research Network, Eötvös Loránd University, Budapest 1117, Hungary
[3]Department of Ecology, University of Veterinary Medicine Budapest, Budapest 1078, Hungary
[4]Laboratory of Endocrine Neurobiology, Institute of Experimental Medicine, Eötvös Loránd Research Network, Budapest 1083, Hungary
[5]Tamás Roska Doctoral School, Péter Pázmány Catholic University, Budapest 1083, Hungary
[6]Laboratory of Reproductive Neurobiology, Institute of Experimental Medicine, Eötvös Loránd Research Network, Budapest 1083, Hungary
[7]Department of Behavioral and Stress Studies, Institute of Experimental Medicine, Eötvös Loránd Research Network, Budapest 1083, Hungary
[8]Centre for Neuroscience, Szentágothai Research Centre, Institute of Physiology, Medical School, University of Pécs, Pécs 7624, Hungary
[9]Human Brain Tissue Bank, Semmelweis University, Budapest 1094, Hungary
[10]Department of Neuropeptide Research in Psychiatry, Central Institute of Mental Health, University of Heidelberg, Mannheim 68159, Germany
[11]Systems Neuroscience Imaging Resource, National Institute of Mental Health, NIH, Bethesda, MD 20892, USA
[12]Laboratory of Brain Circuits Therapeutics, Achucarro Basque Center for Neuroscience, Leioa, Spain
[13]Ikerbasque – Basque Foundation for Science, Bilbao, Spain
[14]Lead contact
*Correspondence: valery.grinevich@zi-mannheim.de (V. G.), dobolyi.arpad@ttk.elte.hu (A. D.)
https://doi.org/10.1016/j.cub.2022.08.062

SUMMARY

Social touch is an essential component of communication. Little is known about the underlying pathways and mechanisms. Here, we discovered a novel neuronal pathway from the posterior intralaminar thalamic nucleus (PIL) to the medial preoptic area (MPOA) involved in the control of social grooming. We found that the neurons in the PIL and MPOA were naturally activated by physical contact between female rats and also by the chemogenetic stimulation of PIL neurons. The activity-dependent tagging of PIL neurons was performed in rats experiencing physical social contact. The chemogenetic activation of these neurons increased social grooming between familiar rats, as did the selective activation of the PIL-MPOA pathway. Neurons projecting from the PIL to the MPOA express the neuropeptide parathyroid hormone 2 (PTH2), and the central infusion of its receptor antagonist diminished social grooming. Finally, we showed a similarity in the anatomical organization of the PIL and the distribution of the PTH2 receptor in the MPOA between the rat and human brain. We propose that the discovered neuronal pathway facilitates physical contact with conspecifics.

INTRODUCTION

Social touch is a major component of social interactions. It is important in both sexual and nonsexual contexts in humans.[1] In rodents, where modes of communication between conspecifics are more limited, the role of social touch may be even more pronounced, as part of the stereotypic behavioral repertoire for social interactions between individuals.[2] The hypothalamus is a major regulatory center of rodent social behavior. It is also likely to be involved in the control of instinctive behaviors in humans.[3] Social sensory inputs are known to reach the cerebral cortex via the thalamus; however, it is not known how information needed for social behavior arrives in the hypothalamus. Although it is possible that information on social context reaches the hypothalamus via the cerebral cortex,[4] it is also conceivable that ascending sensory pathways carrying information on social touch might project directly to the hypothalamus as has been demonstrated recently in zebrafish.[5] Within the responsible neuronal circuits, neuropeptides have been implicated in the control of a variety of social behaviors. Oxytocin, a pro-social neuropeptide, is known to promote social interactions, including social touch in rodents.[6] Other neuropeptides, such as Tac2, were shown to play crucial roles in the behavioral response to chronic social isolation.[7] Parathyroid hormone 2 (PTH2), a peptide originally named tuberoinfundibular peptide of 39 residues (TIP39),[8] was recently demonstrated to sense the presence of conspecifics in zebrafish via mechanoreceptors in the lateral line organ.[9] In mammals, PTH2 expression is known to be elevated in mothers and participates in maternal care, as demonstrated by the decreased motivation of mother rats to contact and suckle their pups after local delivery of a PTH2 receptor (PTH2R) antagonist to the medial preoptic area (MPOA),

Please cite this article in press as: Keller et al., A thalamo-preoptic pathway promotes social grooming in rodents, Current Biology (2022), https://doi.org/10.1016/j.cub.2022.08.062

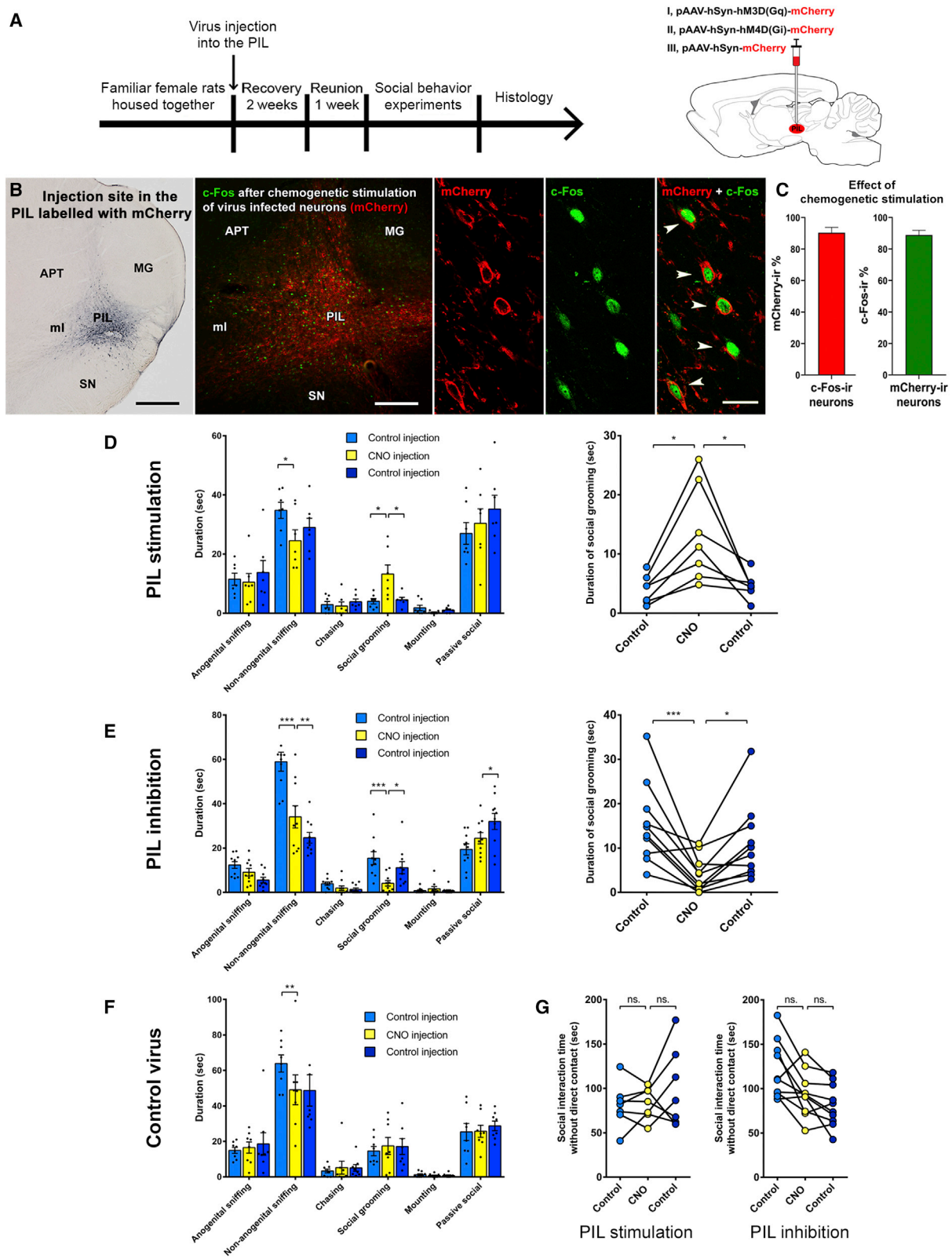

(legend on next page)

CURBIO 18757

Please cite this article in press as: Keller et al., A thalamo-preoptic pathway promotes social grooming in rodents, Current Biology (2022), https://doi.org/10.1016/j.cub.2022.08.062

located in the anterior hypothalamus.[10] PTH2 is expressed in an unusual brain site for a neuropeptide, the thalamus, where few other neuropeptides have been described. Within the thalamus, PTH2 is confined to the posterior intralaminar thalamic nucleus (PIL), a multisensory information processing relay station.[11] Since PTH2 terminals are abundant in the MPOA, the MPOA receives a major PTH2 projection from the PIL based on retrograde tracer studies,[10] and PIL PTH2 neurons increased their activity in response to social interaction,[12] we hypothesized that PTH2 neurons convey social inputs to the MPOA. To test this hypothesis, we examined the effect of chemogenetic-based stimulation of PIL neurons tagged by social contact experience. This stimulation promoted social grooming between same-sex individuals. Among the projection sites of the PIL identified by anterograde viral tracing, only the MPOA was exclusively activated by direct social interaction, and in turn, the selective stimulation of the PIL→MPOA pathway elevated social grooming between the animals. To elucidate the role of PTH2 present in the pathway, we investigated its expression in response to social interaction. We found that it was increased. It was previously shown that PTH2R[13] is present in the MPOA, and we now found that PTH2 increases the activity of MPOA neurons while antagonizing PTH2 selectively inhibited social grooming. Thus, we have identified a direct, PTH2-containing pathway, which controls social grooming behavior independently from the established thalamo-cortical circuits.

RESULTS

Stimulation of PIL elicits social grooming in rats

The effect of the chemogenetic manipulation of PIL neurons

To investigate whether PIL manipulation affects social behaviors, we injected excitatory (recombinant adeno-associated virus [rAAV]-**P**$_{hSYN}$-hM3D(Gq)-mCherry) or inhibitory (pAAV-**P**$_{hSYN}$-hM4D(Gi)-mCherry) designer receptor exclusively activated by the designer drug (DREADD)-expressing or control viruses (rAAV-**P**$_{hSYN}$-mCherry) into the PIL of female rats. The animals were subsequently housed individually for 2 weeks and then reunited for 1 week (Figure 1A) prior to injection of clozapine-N-oxide (CNO), the agonist of the DREADD. Almost all (90.4% ± 3.4%) activated cells contained mCherry and almost all (88.9% ± 3.0%) mCherry-positive neurons in the PIL showed c-Fos-positivity 1.5 h after CNO administration, which validates the effectiveness of our chemogenetic stimulation (Figures 1B and 1C).

Next, we investigated several distinct social behavioral elements during the 10 min following the activation or inhibition of PIL neurons. The duration of social grooming significantly increased upon the chemogenetic stimulation compared with the previous day and also compared with vehicle injection on the following day (Figure 1D). In turn, the inhibition of the PIL neurons reduced grooming compared with the control days (Figure 1E). In the absence of a DREADD, the viral infection and the CNO administration did not affect social grooming (Figure 1F). Note that the stimulation and the inhibition of PIL neurons have the opposite effect on social grooming, whereas other behavioral elements were not affected by the manipulation or changed in the same direction following the different treatments (e.g., non-anogenital sniffing).

In the next experiment, direct contact between the animals was prevented by separating them by a bar wall allowing them to smell, hear, and see each other. The chemogenetic activation of the PIL had no effect on the duration of social interaction under these conditions, highlighting the importance of the PIL in forming direct contact (Figure 1G).

The chemogenetic manipulation of the PIL was repeated in male rats as well with the same results (Figure S1A). Namely, the duration of social grooming increased following stimulation and decreased following the inhibition of PIL neurons (Figures S1B and S1D), whereas the control virus had no behavioral effect on the animals (Figure S1F). Furthermore, the manipulation of PIL neurons had no effect on the behavior of the subjects when physical contact between the animals was prevented (Figures S1C, S1E, and S1G).

Manipulation of PIL neurons, which were activated during a previous social encounter

To selectively manipulate PIL neurons activated by social exposure, we used the virus-delivered genetic activity-induced tagging of cell ensembles (vGATE) method.[14] Excitatory, inhibitory, and control viral cocktails (rAAV-(tetO)$_7$-**P**$_{fos}$-rtTA; rAAV-**P**$_{tet}$bi-Cre/YC3.60; rAAV-**P**$_{hSYN}$-DIO-hM3D(Gq)-mCherry/rAAV-**P**$_{hSYN}$-DIO-hM4D(Gi)-mCherry/pAAV-**P**$_{hSYN}$-DIO-mCherry) were injected into the PIL of female rats. In the vGATE system, a c-Fos promoter

Figure 1. Effect of chemogenetic manipulation of PIL on social grooming in female rats

(A) Experimental protocol of the chemogenetic manipulation of the PIL in female rats.

(B) The PIL as the injection site of the virus expressing mCherry fluorescent tag and the *in vivo* validation of the effectiveness of chemogenetic stimulation. The PIL is located in the posterior part of the thalamus in rats, the dorsal from the SN, and the ventromedial from the MG. DREADD-expressing mCherry-immunopositive neurons (red) colocalized with c-Fos (green) in response to CNO injection. Scale bars, 750 (left), 300 (middle), and 60 μm (right).

(C) Quantification of CNO-induced c-Fos expression in the PIL. Most of the c-Fos-expressing cells were mCherry positive, while most of the mCherry-positive neurons were activated after the injection of CNO, n = 6.

Q9 (D) Chemogenetic stimulation of PIL neurons in freely moving adult females. N = 7, repeated-measures ANOVA followed by Šídák's multiple comparisons tests, for social grooming: p = 0.028 (1st control versus CNO) and p = 0.041 (CNO versus 2nd control).

(E) Chemogenetic inhibition of PIL neurons in freely moving adult females. N = 10, repeated-measures ANOVA followed by Šídák's multiple comparisons tests, for social grooming: p = 0.0005 (1st control versus CNO) and p = 0.0495 (CNO versus 2nd control).

(F) The absence of effect of control virus on the social interaction in freely moving adult females. N = 8, repeated-measures ANOVA followed by Šídák's multiple comparisons tests, for social grooming: p = 0.88 (1st control versus CNO) and p = 0.99 (CNO versus 2nd control).

(G) Chemogenetic stimulation and inhibition of PIL in absence of physical contact. For stimulation (n = 7), one-way ANOVA followed by Šídák's multiple comparisons tests, p = 0.99 (1st control versus CNO) and p = 0.64 (CNO versus 2nd control); for inhibition (n = 10), one-way ANOVA followed by Šídák's multiple comparisons tests, p = 0.072 (1st control versus CNO) and p = 0.14 (CNO versus 2nd control). 0.010 < *p < 0.050, 0.001 < **p < 0.010 and ***p < 0.001. Values are mean ± SEM.

See also Figure S1.

Please cite this article in press as: Keller et al., A thalamo-preoptic pathway promotes social grooming in rodents, Current Biology (2022), https://doi.org/10.1016/j.cub.2022.08.062

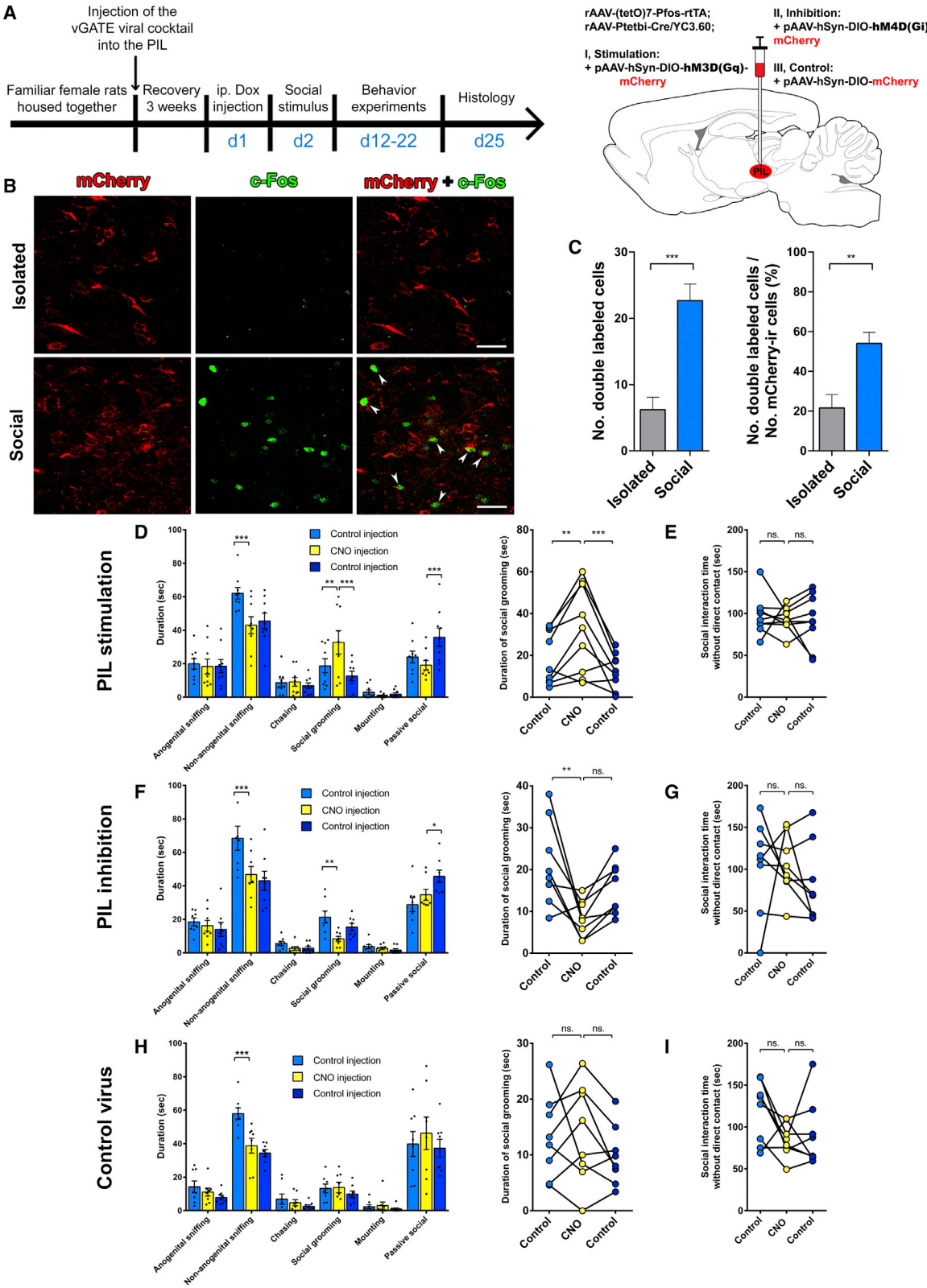

(legend on next page)

CURBIO 18757

Please cite this article in press as: Keller et al., A thalamo-preoptic pathway promotes social grooming in rodents, Current Biology (2022), https://doi.org/10.1016/j.cub.2022.08.062

($\mathbf{P}_{fos}$) fragment drives the expression of the reverse tetracycline sensitive (tet) transactivator (rtTA). Following the recovery of the animals, a single intraperitoneal (i.p.) doxycycline (Dox) administration launched the autoregulatory expression loop of $(tetO)_7$-rtTA, thus opening the labeling period. The following day, the subjects were reunited with a cagemate in their home cage for 2 h as direct social exposure, which resulted in the expression of the DREADD or control sequence in social contact experienced vGATE-tagged neurons only (encoded in the third virus: rAAV-$\mathbf{P}_{hSYN}$-DIO-hM3D(Gq)-mCherry, rAAV-$\mathbf{P}_{hSYN}$-DIO-hM4D(Gi)-mCherry or rAAV-$\mathbf{P}_{hSYN}$-DIO-mCherry) (Figure 2A). Social behavior experiments were conducted 10 days later (during which the animals were kept in isolation), and then the brains were processed for histological analysis. Animals in diestrus were used for behavioral experiments.

The labeling of calcium-binding proteins revealed that the PIL region infected with the vGATE viruses was surrounded by parvalbumin-positive cells and that the vast majority of the calbindin-positive cells were vGATE labeled (90.6%; n = 3; Figure S2B), an established characteristic of PTH2 neurons.[12,15] To validate the applied vGATE method, we performed c-Fos immunolabeling after direct social exposure or isolation (Figure 2B). After social exposure, 2.4 times more cells were labeled for c-Fos (32.2 ± 4.0; n = 3) than after isolation (13.4 ± 4.3; n = 2), which is a significant difference (two-tailed unpaired t test, p = 0.011). mCherry double labeling was found in 72.8% ± 6.4% of the c-Fos-ir cells (representing vGATE-labeled neurons) in the social group compared with 38.2% ± 10.2% in the isolated group (two-tailed unpaired t test, p = 0.015). In addition, 54.0% ± 5.5% of the mCherry cells were double labeled with c-Fos after social interaction compared with 21.5% ± 6.7% after isolation (two-tailed unpaired t test, p = 0.0044; Figure 2C).

During the direct contact social behavior test, where the animals could freely interact with each other, the duration of social grooming significantly increased following the stimulation (Figure 2D) and, in turn, decreased following the inhibition of vGATE-tagged PIL neurons (Figure 2F). Furthermore, no behavioral changes were found in the group injected with the control virus (Figure 2H). Notably, only direct physical contact elicited an increase in social interaction time after chemogenetic manipulation of vGATE-tagged PIL neurons (Figures 2E, 2G, and 2I).

We performed a control experiment for the vGATE protocol in which the day following the i.p. Dox injection, the animals remained isolated and received no social stimulus (Figures S2A and S2B). As predicted, since the virus was expressed in socially tagged neurons, the excitatory vGATE viral cocktail had no effect on the social behavior of the animals during the freely moving social interaction test (Figure S2C).

The locomotor effect of CNO injection was excluded by an open-field test. Indeed, the total distance covered by the animals was not affected by the manipulation of PIL neurons, suggesting that the altered social behaviors were not a consequence of altered locomotor drive (Figure S2D).

Social behaviors initiated by the stimulus animals were also examined. In contrast to the changes in social behavior after the manipulation of socially tagged PIL neurons in the experimental animals, the social interactions initiated by the untreated stimulus animals were not affected (Figure S2E).

The ineffectiveness of chemogenetic manipulation of PIL neurons on the performance of female and male animals during the social novelty preference test (Figure S3) implies that the function of the PIL is specific to the regulation of social grooming.

Projections of the PIL and the activation of its target area during direct contact social behavior in rats

To determine neuronal connections of PIL neurons, the anterograde tracer biotinylated dextran amine (BDA) was injected into the PIL of female rats (Figures 3A and 3B). Labeled axons were found in a number of socially relevant brain regions, such as the infralimbic cortex (ILC), lateral septum (LS), medial preoptic nucleus (MPN), MPOA, ventral bed nucleus of stria terminalis (vBNST), paraventricular hypothalamic nucleus (PVN), medial amygdala (MeA), dorsomedial hypothalamic nucleus (DMH), periaqueductal central gray (PAG), and lateral parabrachial nucleus (LPB) (Figures 3C and 3D; Table S1). A further aim was to find out whether social interaction activates the target areas of the PIL together with the activation of the PIL itself, which was reported previously[12] and confirmed in this study (Figures S4A–S4C). We found four brain regions, the ILC,

Figure 2. Effects of the manipulation of PIL using vGATE viral cocktail

(A) Experimental protocol of the chemogenetic PIL manipulation using vGATE viruses.

(B) *In vivo* validation of the vGATE technique: neurons infected by the vGATE viruses were activated after social exposure (indicated by white arrowheads) but not in isolated control animals. Scale bars, 75 μm.

(C) Quantification of social-induced c-Fos expression in the vGATE-tagged PIL. Significantly more cells were labeled for c-Fos after social exposure than after isolation. In addition, significantly more mCherry cells were double labeled with c-Fos after social interaction compared with the number of cells labeled after isolation.

(D) vGATE stimulation of PIL neurons in freely moving adult females. N = 9, repeated measures-ANOVA followed by Šídák's multiple comparisons tests, for social grooming: p = 0.0019 (1st control versus CNO) and p < 0.001 (CNO versus 2nd control).

(E) vGATE stimulation of PIL in absence of physical contact. N = 9, one-way ANOVA followed by Šídák's multiple comparisons tests, p = 0.96 (1st control versus CNO) and p = 0.99 (CNO versus 2nd control).

(F) vGATE inhibition of PIL neurons in freely moving adult females. N = 8, repeated-measures ANOVA followed by Šídák's multiple comparisons tests, for social grooming: p = 0.0018 (1st control versus CNO) and p = 0.16 (CNO versus 2nd control).

(G) vGATE inhibition of PIL in absence of physical contact. N = 8, one-way ANOVA followed by Šídák's multiple comparisons tests, p > 0.99 (1st control versus CNO) and p = 0.46 (CNO versus 2nd control).

(H) The effect of vGATE control virus on the social interaction in freely moving adult females. N = 8, repeated-measures ANOVA followed by Šídák's multiple comparisons tests, for social grooming: p = 0.99 (1st control versus CNO) and p = 0.69 (CNO versus 2nd control).

(I) The effect of vGATE control virus on social interaction in absence of physical contact. N = 8, one-way ANOVA followed by Šídák's multiple comparisons tests, p = 0.14 (1st control versus CNO) and p = 0.95 (CNO versus 2nd control). 0.010 < *p < 0.050, 0.001 < **p < 0.010 and ***p < 0.001. Values are mean ± SEM. See also Figure S2.

Please cite this article in press as: Keller et al., A thalamo-preoptic pathway promotes social grooming in rodents, Current Biology (2022), https://doi.org/10.1016/j.cub.2022.08.062

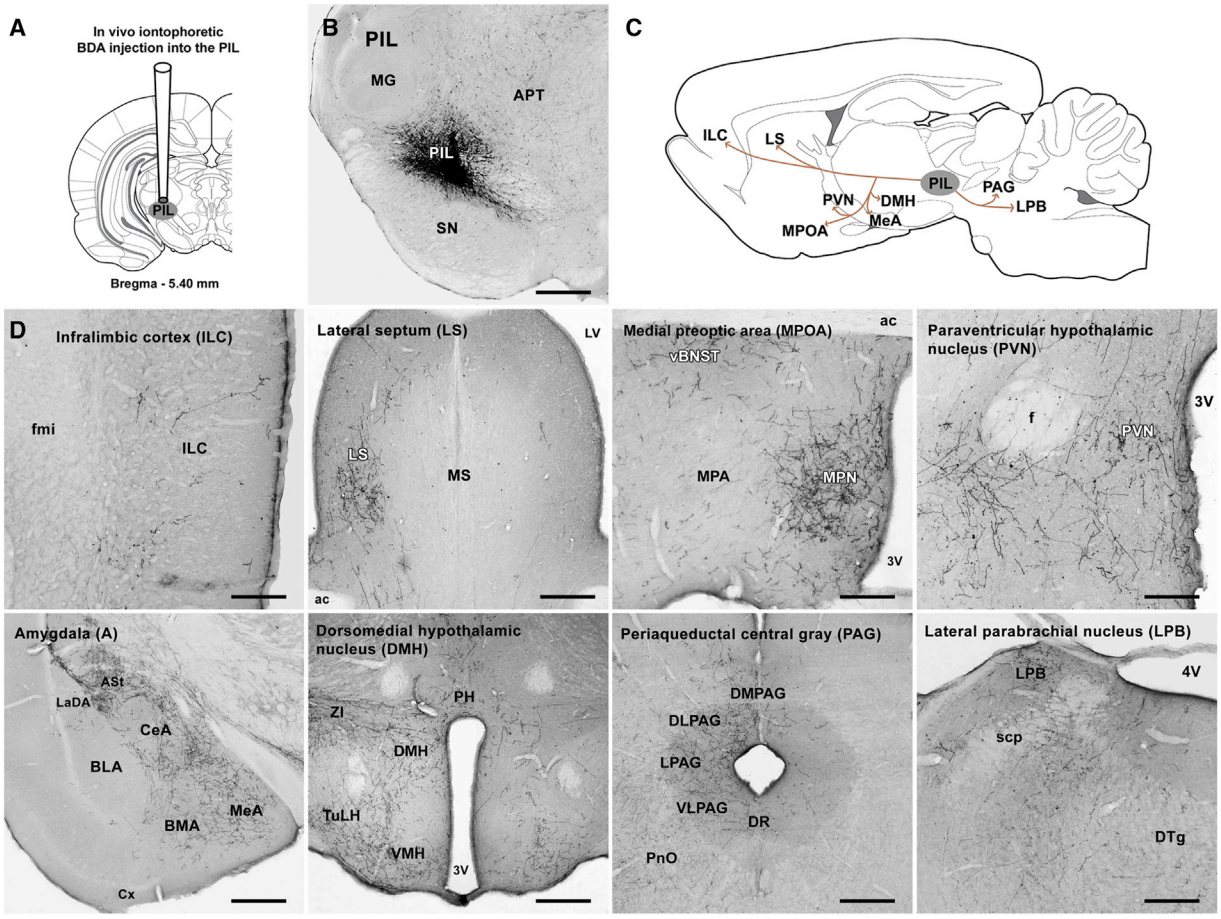

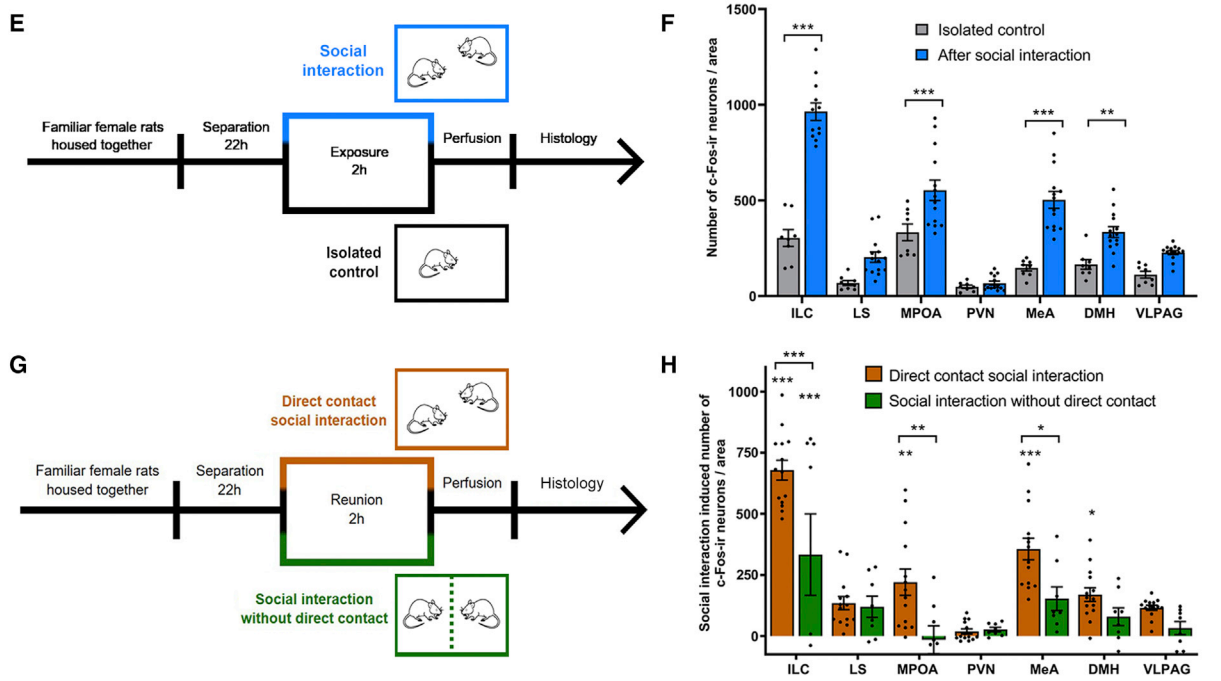

(legend on next page)

CURBIO 18757

Please cite this article in press as: Keller et al., A thalamo-preoptic pathway promotes social grooming in rodents, Current Biology (2022), https://doi.org/10.1016/j.cub.2022.08.062

MPOA, MeA, and DMH, where the numbers of activated neurons were significantly higher after reuniting the rats after 1 week of social isolation as compared with isolated animals (Figure 3F).

We also examined the anterograde transport of the rAAV-$\mathbf{P}_{hSYN}$-hM3D(Gq)-mCherry virus, which was used to stimulate the PIL. mCherry-positive axons had the same distributional pattern as that found by traditional anterograde tracing (Figure S5A), which verifies the accuracy of both the injection sites and the anterograde transport of the virus. Based on the density of the labeled axons, the MPOA and MeA appeared to be the main target areas of the PIL. Following control injections of the virus into the adjacent substantia nigra (SN), the labeled fibers were present only in the caudate putamen and not in the target areas of the PIL (Figure S5B).

In the chemogenetic experiment, the administration of CNO without social stimuli resulted in c-Fos activation in the PIL and also in socially relevant target areas of PIL neurons in a pattern similar to that detected after social interaction. A significantly higher number of c-Fos-positive neurons was found in the PIL, due to the direct effect of the chemogenetic stimulation, and in the PIL targets ILC, MPOA, and MeA, compared with vehicle injection (Figures S4D–S4F).

The effect of direct physical contact was also determined in PIL target areas by comparing freely interacting rats with ones separated by bars (Figure 3G). Three brain regions were identified in which the number of activated neurons was significantly lower when physical contact was prevented: the ILC, MPOA, and MeA (Figure 3H). With the exclusion of physical contact, the activation of the MPOA was similar to the control animals, without any social stimulus, highlighting the importance of direct contact in the activation of this particular region. Notably, one of the highest densities of PIL neuron axonal terminals was found in the MPOA (Figure S4A), and the activation of this area seemed to be specifically related to direct social contact, so we further investigated the role of the PIL→MPOA circuit.

Projections of PIL neurons to the MPOA facilitate the behavioral effect of physical contact

A retrogradely transported virus expressing Cre-recombinase and mCherry fluorescent protein was injected into the MPOA. Three weeks later, a Cre-dependent virus expressing mCitrine and an excitatory or inhibitory DREADD was injected into the PIL (Figures 4A and 4B). As demonstrated by the expression of mCherry and mCitrine, respectively, the MPOA injected Cre-recombinase expressing virus spread to afferent brain areas including the PIL, and the Cre-dependent mCitrine fluorescent protein and associated DREADD were expressed only in MPOA-projecting PIL neurons. During the freely moving social behavior experiment, the selective chemogenetic stimulation of MPOA-projecting PIL neurons did not increase the duration of social grooming (Figure 4C), but the selective chemogenetic inhibition of MPOA projecting PIL neurons decreased the duration of social grooming (Figure 4D) following the i.p. CNO administration. Chemogenetic stimulation of PIL axonal terminals in the MPOA was also performed using local delivery of CNO into the MPOA (Figure 4E). The chemogenetic activation of axonal terminals of PIL neurons in the MPOA increased the duration of social grooming of the experimental animal (Figure 4F).

Characteristics of PTH2-sensitive preoptic neurons

We observed that GABAergic cells in the MPOA were activated after social exposure. PTH2-containing fibers were abundant in the MPOA, with a distribution similar to that of socially activated neurons (Figure 5A). Therefore, we investigated the connection between the GABAergic neurons in the MPOA and the PTH2 neuropeptide and found that MPOA GABAergic cells were closely apposed by PTH2-containing fibers (Figure 5B).

PTH2 acts on PTH2R. The visualization of this receptor in PTH2R-ZsGreen mice confirmed its presence in the MPOA. Furthermore, social interaction activated these cells, which was demonstrated by an increased number of MPOA c-Fos positive PTH2R-expressing neurons (Figure 5C).

The PTH2→GABAergic MPOA connection was further demonstrated by the acute slices patch-clamp technique. The GABAergic MPOA neurons of female VGAT-ZsGreen mice were activated by PTH2 confirmed by dose-dependent transient elevations in their firing rate while an antagonist of the PTH2R eliminated this action (Figures 5D and 5E).

Finally, we performed an experiment infusing PTH2R antagonist into the lateral ventricle of female rats via osmotic minipumps (Figure 5F). The results demonstrate an important role of PTH2 in the control of social grooming because this behavioral element

Figure 3. Anterograde projections of the PIL and activation of PIL target area neurons upon social interaction with or without direct physical contact between the female rats

(A) Injection of the anterograde tracer BDA into the PIL.

(B) A representative BDA injection site in the PIL. Scale bars, 750 μm.

(C) Summary of the projections of PIL neurons based on anterograde tract tracing.

(D) Anterogradely labeled fibers are shown in several brain regions implicated in social behavior, such as the ILC, LS, MPOA, PVN, amygdala, dorsomedial and some other hypothalamic nuclei, PAG, and some pontine structures, including the LPB. Scale bars, 300 (ILC and PVN), 375 (MPOA), 450 (LPB), 600 (LS), and 750 μm (MeA, DMH, and PAG).

(E) Experimental protocol for studying activation of target areas of the PIL upon freely moving social encounters.

(F) Comparison of the c-Fos activation of seven socially implicated brain regions. For isolated control group, n = 8; for social interaction, n = 14, two-way ANOVA followed by Šídák's multiple comparisons tests; for ILC, $p < 0.001$; for LS, $p = 0.056$; for MPOA, $p < 0.001$; for PVN, $p = 0.99$; for MeA, $p < 0.001$; for DMH, $p = 0.0067$; for PAG, $p = 0.15$; $0.001 < **p < 0.010$ and $***p < 0.001$. Values are mean ± SEM.

(G) Experimental protocol for studying activation of target areas of the PIL upon social interaction in absence of physical contact.

(H) Comparison of the c-Fos activation of seven socially implicated brain regions. The diagram represents the number of social-interaction-induced c-Fos-ir neurons ([the number of activated neurons after social exposure − number of activated neurons in isolated animals]/area). For direct social interaction, n = 14; for social interaction without direct contact and isolated control group, n = 8, two-way ANOVA followed by Šídák's multiple comparisons tests. Direct contact social interaction versus social interaction without direct contact: for ILC, $p < 0.001$; for LS, $p > 0.99$; for MPOA, $p = 0.0080$; for PVN, $p > 0.99$; for MeA, $p = 0.034$; for DMH, $p = 0.80$; for VLPAG, $p = 0.86$; $0.010 < *p < 0.050$, $0.001 < **p < 0.010$ and $***p < 0.001$. Values are mean ± SEM.

See also Figures S3–S5 and Table S1.

Please cite this article in press as: Keller et al., A thalamo-preoptic pathway promotes social grooming in rodents, Current Biology (2022), https://doi.org/10.1016/j.cub.2022.08.062

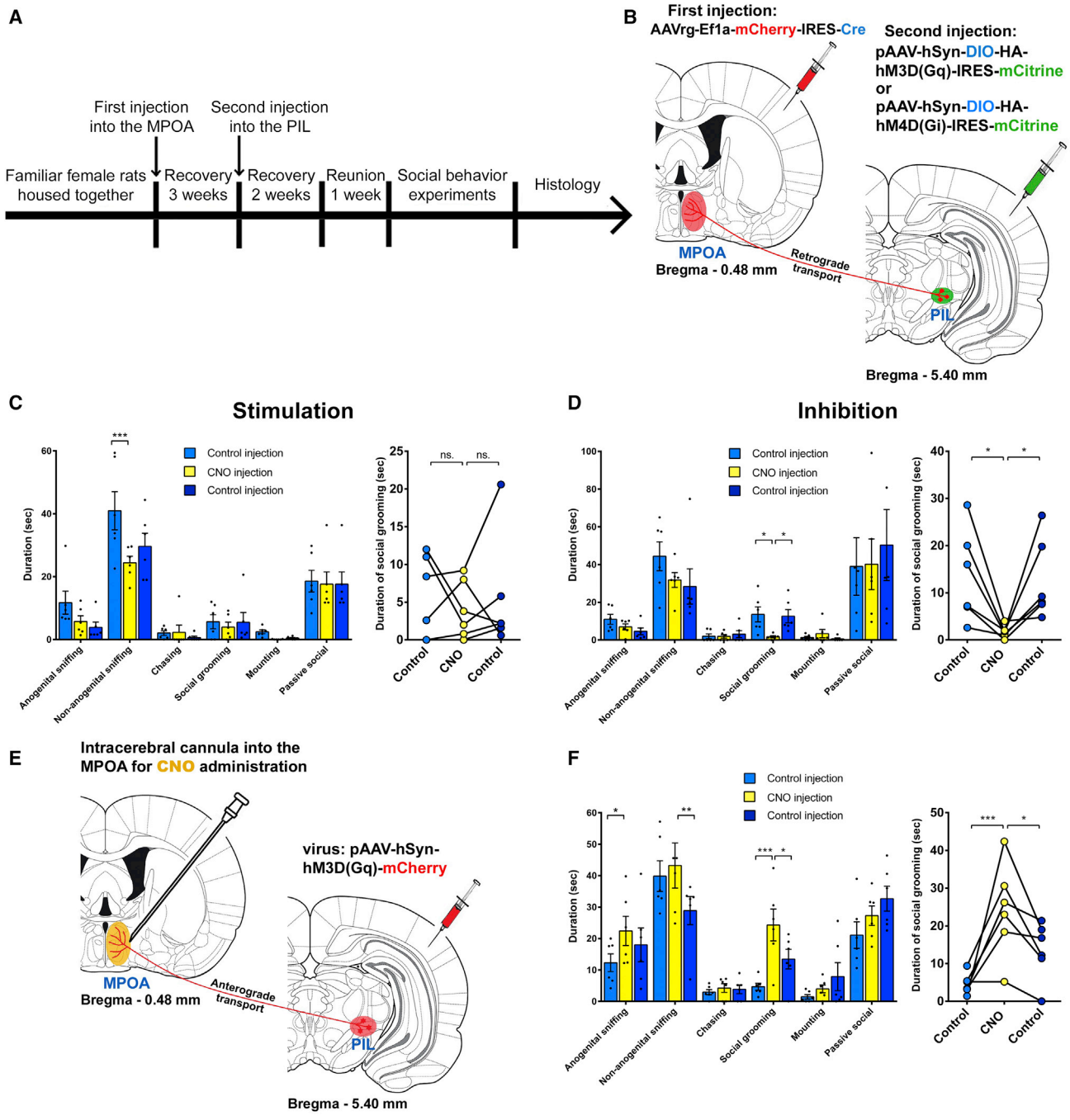

Figure 4. Demonstration of the role of PIL-MPOA projection in social grooming in female rats

(A) Experimental timeline for the selective chemogenetic manipulation of PIL neurons projecting to the MPOA.

(B) Experimental design of the double viral injections.

(C) Stimulation of PIL neurons projecting to MPOA in freely moving animals. N = 6, repeated measures ANOVA followed by Šídák's multiple comparisons tests, for social grooming: $p = 0.92$ (1^{st} control versus CNO) and $p = 0.94$ (CNO versus 2^{nd} control).

(D) Inhibition of PIL neurons projecting to MPOA in freely moving animals. N = 6, Friedman test followed by Dunn's multiple comparisons tests, for social grooming: $p = 0.028$ (1^{st} control versus CNO) and $p = 0.028$ (CNO versus 2^{nd} control).

(E) Experimental design of the stimulation of fiber terminals of PIL neurons in the MPOA with local CNO administration using intracerebral cannula implanted into the MPOA.

(F) The effect of the selective chemogenetic stimulation of fiber terminals of PIL neurons in the MPOA on social behavior. N = 6, repeated measures ANOVA followed by Šídák's multiple comparisons tests, for social grooming: $p < 0.001$ (1^{st} control versus CNO) and $p = 0.029$ (CNO versus 2^{nd} control). $0.010 < *p < 0.050$. $0.010 < *p < 0.050$, $0.001 < **p < 0.010$, and $***p < 0.001$. Values are mean ± SEM.

Please cite this article in press as: Keller et al., A thalamo-preoptic pathway promotes social grooming in rodents, Current Biology (2022), https://doi.org/10.1016/j.cub.2022.08.062

CellPress

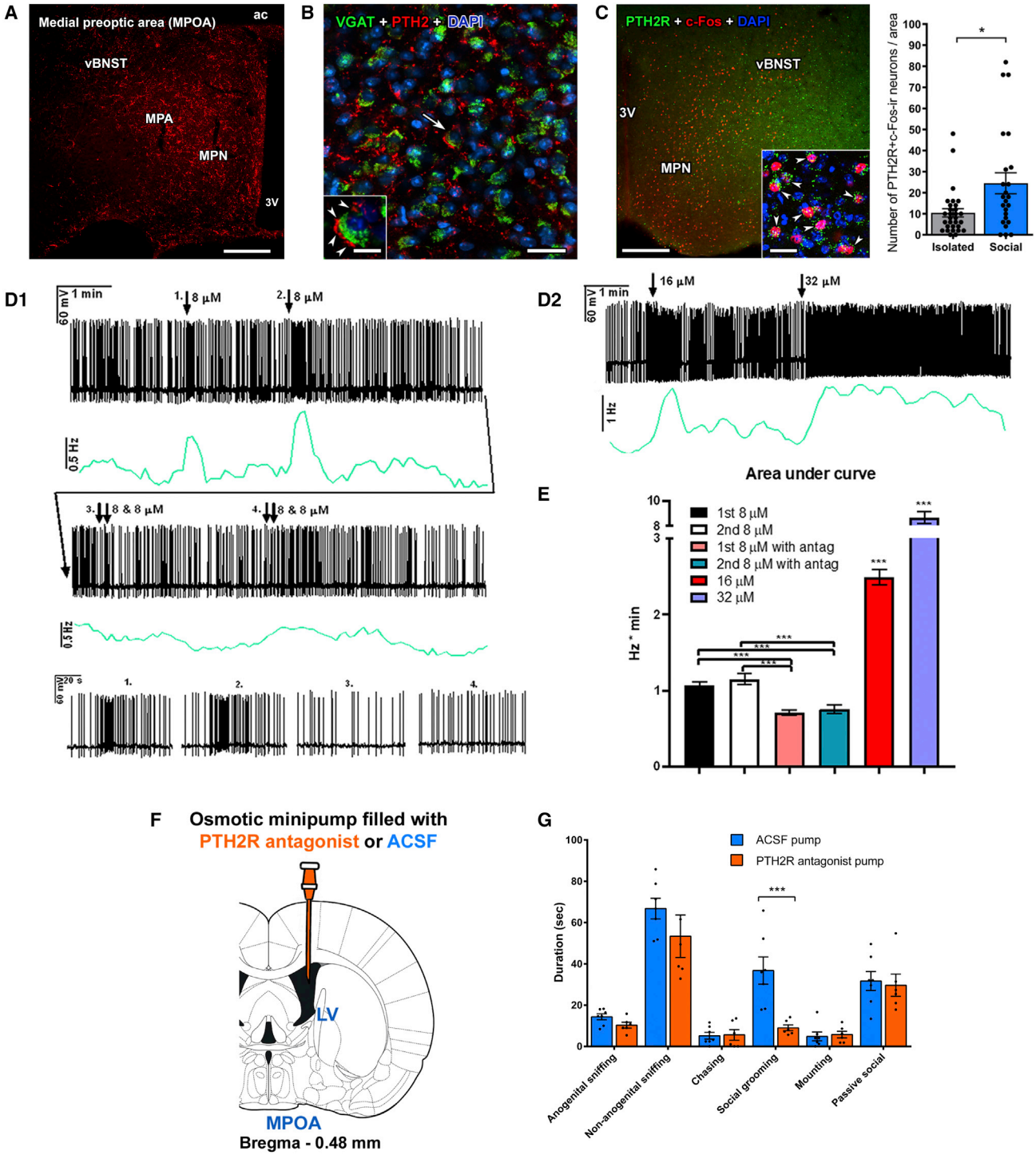

Figure 5. The effect of PTH2 on preoptic neurons

(A) PTH2-positive fibers in the MPOA.

(B) PTH2-ir fibers (red) closely apposed the cell bodies (blue) of VGAT-positive neurons (green) in the MPOA of VGAT-ZsGreen mice. Scale bars, 70 and 50 µm (inset).

(C) The PTH2R (green), the receptor for PTH2, was expressed in c-Fos activated (red) neurons (blue) of the MPOA after social contact in PTH2R-ZsGreen mice. The number of double labeled PTH2R/c-Fos-positive neurons in the MPOA was significantly higher after social interaction with another female conspecific compared with isolated controls. N = 30 for isolated, n = 24 for social, two-tailed unpaired t test, *p = 0.013. Values are mean ± SEM. Scale bars, 300 (main) and 50 µm (inset).

(legend continued on next page)

Please cite this article in press as: Keller et al., A thalamo-preoptic pathway promotes social grooming in rodents, Current Biology (2022), https://doi.org/10.1016/j.cub.2022.08.062

was specifically reduced in the PTH2R antagonist treated group compared with the artificial cerebrospinal (ACSF)-injected control group (Figure 5G).

The PIL and its PTH2-expressing neurons

The exact borders of the PIL, which is located in the thalamus dorsal to the SN and ventromedial to the medial geniculate body (MG) (Figure 6A), were defined using the location of PTH2 neurons as well as calcium-binding proteins. Parvalbumin immunoreactive (-ir) neurons were abundant in brain regions surrounding the PIL, whereas only a few cells were labeled with parvalbumin within the PIL. By contrast, PTH2 appeared exclusively in the PIL, with most of the cells double labeled with calbindin (Figure 6B).

The expression of PIL PTH2 mRNA was 2.4 times higher in animals kept in a social environment (together with conspecifics in their home cage) compared with control animals socially isolated for 2 weeks (Figure 6C).

The PIL and PTH2 receptors in the MPOA in the human brain

To investigate whether the PIL→MPOA circuit observed in rodents also exists in the human brain, we used autopsy material for histological analysis. Using the same calcium-binding proteins that we used to describe the chemo-architecture of the PIL in rodent models, we were able to demonstrate the existence of a corresponding brain region in the human thalamus (Figure 6D). Parvalbumin labeled the surrounding MG but not the PIL, whereas calbindin-positive cells were abundant in the PIL region, indicating the existence of a chemo-architecturally similar PIL in humans. Further histological staining techniques also distinguished the PIL cytoarchitectonically from the surrounding brain regions (Figure 6E). Furthermore, PTH2R immunoreactive neurons were also detected in the human MPOA (Figure 6F).

DISCUSSION

The induction of PTH2 in response to social interaction generalizes previous findings on the elevated level of PTH2 in a mother rat in the presence of her litter.[18] These data are also in line with a recent report that the level of the corresponding peptide, PTH2, in individual zebrafish is proportional to the total density of zebrafish in the surrounding environment.[9] In zebrafish, the cells expressing PTH2 were localized in a domain known to control the specification of diencephalic neuroendocrine cells.[19] The site of socially dependent expression of PTH2 in mammals is the PIL,[20] an area also defined in humans based on molecular anatomy.[21] The PIL corresponds to the area expressing PTH2 in the zebrafish based on the location of the cells. For details of previous anatomical and functional investigations of the PIL area, see Table S2.

Although the zebrafish study established the induction of PTH2 by conspecifics,[9] the actual function and characteristics of PTH2 neurons, and PTH2 itself, remained unexplored. To address this question, we manipulated PIL neurons using chemogenetic tools in rats and found that the time spent with social grooming was increased by chemogenetic stimulation of PIL neurons. The changes were similar in males and females, suggesting similar roles of the network in both sexes despite a higher PTH2 level in females.[22] Other types of social interactions, including sniffing or staying in the vicinity of each other when separated by walls, were not affected. The physiological relevance of our finding is supported by the reduced duration of social grooming following the inhibition of the same PIL neurons. In addition, social recognition and preference for social novelty were also not changed, suggesting a specific role of PIL neurons in direct social contact, without affecting anxiety-like behaviors. In turn, the same increase in the duration of social grooming was found when only those PIL neurons were stimulated chemogenetically, which were activated during a previous social interaction (socially tagged neurons), suggesting that promoting grooming between individuals is dependent on socially activated neurons. Since social touch is rewarding,[23] it is possible that a subset of social contact experienced neurons in the PIL promotes further social contact to maintain social interaction with conspecifics. We have to emphasize that it is not known what stimulus activates PIL neurons during social interactions. The increased number of c-Fos-positive neurons in response to social interaction as well as the detected increase in PTH2 mRNA content could be the result of somatosensory but potentially also auditory or visual inputs. Indeed, we previously demonstrated that auditory input can activate PTH2 neurons of the PIL of rats,[24] whereas visual input activated thalamo-hypothalamic pathways were recently found in the zebrafish.[5]

We showed that PIL neurons project to many brain regions, including the prefrontal cortex, amygdala, and hypothalamus.

(D) (D1) The neuronal activity of MPOA GABAergic neurons in female mice was enhanced by PTH2 in VGAT-ZsGreen mice. The figure shows representative recordings during repetitive PTH2 applications that resulted in transient (less than 1 min) elevations in firing rate. The greenish lines under the recordings represent frequency distribution, presenting two peaks following the applications of PTH2. The recording of the same neuron continued further on (long arrow line). Here, double arrows mark the local application of a PTH2R antagonist immediately before PTH2 (both applied at 8 μM concentration) demonstrating that in the presence of the PTH2R antagonist PTH2 did not have an effect on the activity of the recorded neuron. The four insets in the bottom of the panel are 1 min magnified periods of the recordings, corresponding to the four applications of PTH2 in the absence (1st and 2nd) or in the presence (3rd and 4th) of the PTH2R antagonist. (D2) Higher doses of PTH2 resulted in higher and longer responses, demonstrating dose dependency of PTH2 action on the firing rate of preoptic GABAergic neurons.

(E) Quantitative analysis of PTH2 action on the firing rate of preoptic GABAergic neurons. The effect of local bath application on neuronal activity was calculated as the area under the curve in the frequency distribution. Due to the different durations of the transient effect of the various doses of PTH2, the first four bars (with 8 μM) were calculated with 1 min time window, the 5th bar (16 μM) was calculated with 1.5 min window, and the 6th bar (32 μM) was calculated with 5 min window. Area under curve: 1st 8 μM, 1.17 ± 0.017 Hz*min, n = 9; 2nd 8 μM, 1.24 ± 0.014 Hz*min, n = 9; 1st 8 μM with antagonist, 0.58 ± 0.012 Hz*min, n = 9; 2nd 8 μM with antagonist, 0.61 ± 0.011 Hz*min, n = 9; 16 μM, 2.49 ± 0.103 Hz*min, n = 9; 32 μM, 8.67 ± 0.501 Hz*min, n = 9. Repeated-measures ANOVA was used to examine whether the firing rate change of each group was significant, ***$p < 0.001$. Values are mean ± SEM.

(F) Experimental design of infusion of an antagonist of the PTH2 receptor into the lateral ventricle of female rats using osmotic minipumps.

(G) The effect of the PTH2 receptor antagonist on the social behavior of freely moving animals. N = 7 for ACSF and n = 6 for PTH2R antagonist, repeated-measures ANOVA followed by Šídák's multiple comparisons tests, for social grooming: $p < 0.001$. ***$p < 0.001$. Values are mean ± SEM.

Please cite this article in press as: Keller et al., A thalamo-preoptic pathway promotes social grooming in rodents, Current Biology (2022), https://doi.org/10.1016/j.cub.2022.08.062

CellPress

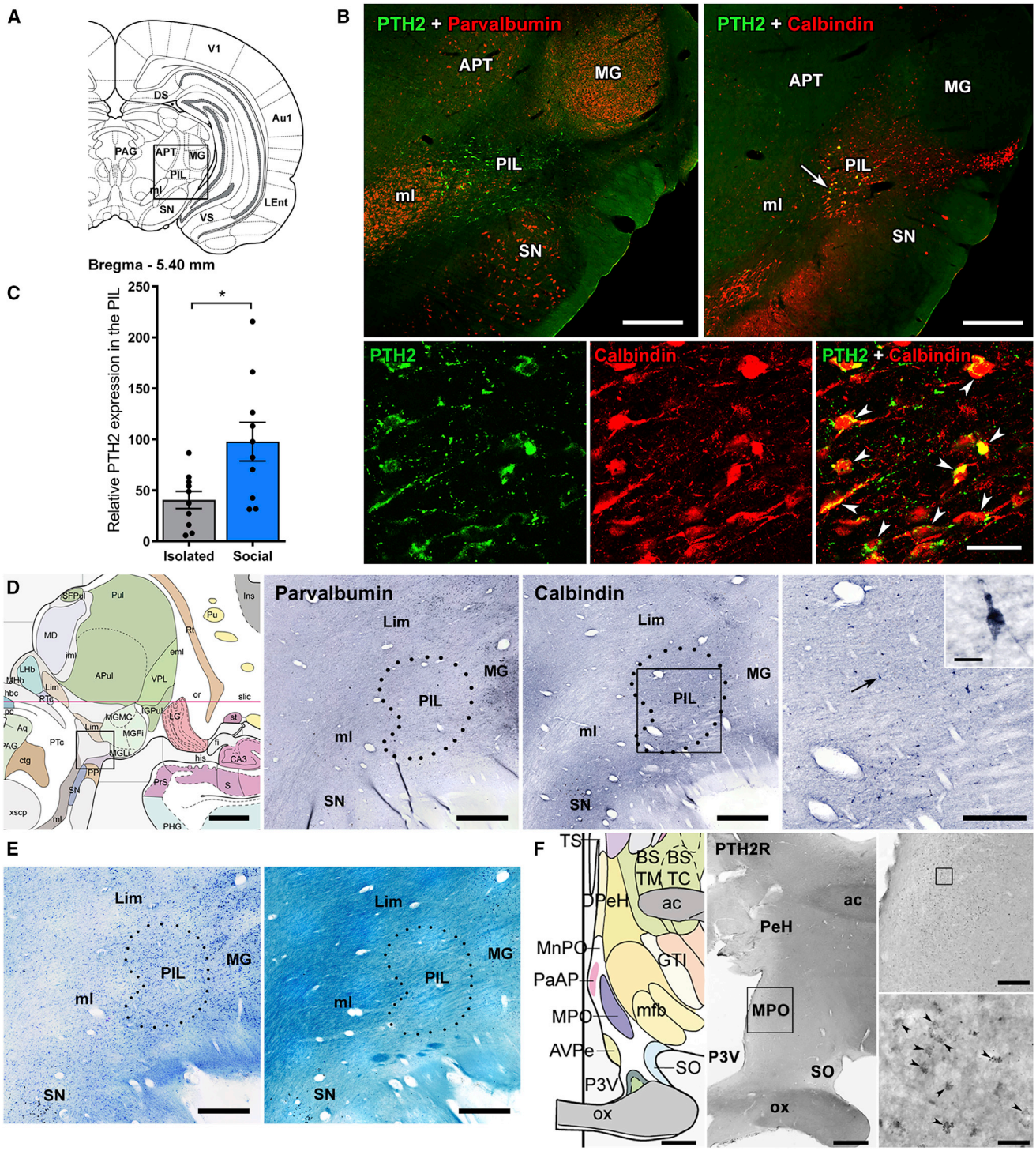

Figure 6. PTH2 content of PIL neurons and elements of the PIL-MPOA pathway in the human brain

(A) The PIL is located in the posterior part of the thalamus in rats, the dorsal from the SN, and the ventromedial from the MG as shown in a drawing of the rat brain.[16]

(B) Chemo-architecture of the PIL in the rat. Neurons in the PIL but not outside of it highly expressed the neuropeptide PTH2 (green). There were only a few parvalbumin-positive neurons (red; upper left panel) in the PIL, whereas parvalbumin-positive neurons were present in several surrounding brain areas, such as the anterior pretectal area (APT), the MG, and the SN. In turn, calbindin-positive neurons (red; upper right and lower panels) were abundant in the PIL. Their distribution overlapped with that of the PTH2 neurons. High-magnification confocal imaging demonstrated that PTH2 and calbindin are co-expressed in the PIL neurons (indicated by white arrowheads). Scale bars, 750 and 100 μm.

(legend continued on next page)

Please cite this article in press as: Keller et al., A thalamo-preoptic pathway promotes social grooming in rodents, Current Biology (2022), https://doi.org/10.1016/j.cub.2022.08.062

The target regions of PIL neurons were similar to the location of PTH2 fibers in the brain,[25] suggesting that PTH2 neurons are the major projection neurons of the PIL, although the presence of other types of projection neurons in the PIL cannot be excluded. Social interaction activated PTH2 neurons in the PIL as well as their target areas. Since social interaction and chemogenetic stimulation of PIL neurons activated the same target areas, we suggest that PTH2 neurons play an important role in conveying the effect of social interactions to a variety of forebrain areas implicated in social behavior. Here, we showed by pathway-specific chemogenetic manipulations that the PIL projections to the MPOA are critical for the mediation of social grooming. In support of this idea, we showed that PTH2-containing terminals closely apposed socially activated PTH2R-expressing GABAergic neurons in the MPOA, whereas antagonizing PTH2R reduced the duration of social grooming. Since retrograde tracer injection into the MPOA labeled the majority of PTH2 neurons in the PIL but not any PTH2 neurons in the other 2 brain sites of PTH2 expression, the subparafascicular area and the lateral paralemniscal nucleus, respectively,[10] we suggest that MPOA PTH2-containing terminals originate in the PIL. On the other hand, we must also emphasize that the actual release of PTH2 has not been demonstrated in this study or previous studies. However, PTH2 was shown in presynaptic terminals innervating MPOA neurons,[15] and our present *in vitro* studies confirmed that MPOA GABAergic cells can be dose-dependently activated by PTH2, making it very likely that PTH2 is released in the MPOA upon proper stimulus.

In conclusion, we discovered a novel subcortical pathway originating from PIL PTH2 neurons and projecting mainly to MPOA GABAergic neurons, which is exclusively activated by social touch and which in turn further promotes social grooming interactions. The activity of this PIL→MPOA pathway and its neuropeptide transmitter, PTH2, may be crucial for a variety of behaviors, including grooming, consolation, and other nonsexual social touch, and potentially also for reproductive behaviors, such as copulation, pair formation, and maternal care in rodents.[26] The findings can be relevant to pathophysiological mechanisms underlying the avoidance of direct physical contact/social touch with conspecifics, a core symptom of autism spectrum disorder.[27] Therefore, the pathway as well as the PTH2 neuropeptide and its receptor should be investigated in the future in disorders where deficits in direct social interactions are found.[28]

STAR★METHODS

Detailed methods are provided in the online version of this paper and include the following:

SUPPLEMENTAL INFORMATION

Supplemental information can be found online at https://doi.org/10.1016/j.cub.2022.08.062.

ACKNOWLEDGMENTS

Support was provided by Hungarian National Research, the Development and Innovation Office (OTKA K134221 and NKFIH-4300-1/2017-NKP_17-00002), the Eötvös Loránd UniversityThematic Excellence Programme 2020 (TKP2020-IKA-05), and the National Brain Program of theHungarian Academy of Sciences 2022 (NAP3) for A.D.; the Gedeon Richter Plc. Centenary Foundation (Gyömrői út 19-21. Budapest, 1103), the Boehringer Ingelheim Funds travel grant, the Excellence Program of theSemmelweis University, the New National Excellence Program of theMinistry of Innovation and Technology, the Doctoral Student Scholarship Program of the Co-operative Doctoral Program of theMinistry of Innovation, and the technology financed from the National Research, Development, and Innovation Office for D.K.; EFOP-3.6.3-VEKOP-16-2017-00009 for D.K. and T.L.; the János Bolyai Research Scholarship of the Hungarian Academy of Sciences for M.C.; NIMH ZIC MH002963-05 for T.B.U.; 2017-1.2.1-NKP-2017-00002 for M.P.; the Ministry of Economy and Business(MINECO) under the framework of the ERA-NET Neuron Cofund and Ministerio Economia, Industria, y Competitividad (Spain) and FEDER (grant RTI2018-101624-B-I00) for M.T.H.; and the German Research Foundation (DFG) (grants GR 3619/8-1, GR 3619/13-1, GR 3619/15-1, and GR 3619/16-1), the Training Research Group (GRK)2174, and the SFB Consortium 1158-2 for V.G. We also appreciate the technical assistance of Nikolett Hanák, Viktória Dellaszéga-Lábas, and Szilvia Deák and the advice of Alan Kania in the behavior analysis.

(C) Significantly higher PTH2 expression was present in the PIL in animals kept in a social environment in comparison with isolated controls, using qRT-PCR. The mRNA level of PTH2/mRNA level of housekeeping genes * 10^6, n = 10 (each group), two-tailed unpaired t test, *p = 0.013. Values are mean ± SEM.
(D) The left panel shows a drawing of the PIL region in humans,[17] from which the framed area is enlarged in subsequent panels. Using calcium-binding proteins as markers, the location of the PIL was identified in the human thalamus. Parvalbumin intensely labeled the adjacent medial geniculate body but not the PIL, whereas calbindin appeared in the PIL but not in the MG. Scale bars, 500 (first image), 100 (second and third images), 40, and 20 μm (fourth image and its inset).
(E) Further histological staining using Nissl (left) and Luxol (right) also indicates the location of the PIL and how it is distinct from the surrounding brain regions. Scale bars, 100 μm.
(F) The expression of PTH2R, the receptor for PTH2, is demonstrated in the human medial preoptic area (indicated by black arrowheads). Scale bars, 2 mm (first two images), 300 μm (third upper image), and 30 μm (third lower image).

AUTHOR CONTRIBUTIONS

D.K. participated in the design of the experiments, performing the behavioral and histological work, interpretation of the results and literature, and writing of the manuscript. T.L. did some of the behavioral studies. M.C., G.P., and J.B. did some of the histological labeling and analysis. V.C. and I.F. performed the patch-clamp experiment. D.Z. did the virus injections into mice. F.D. and M.P. collected the human brain tissue. T.B.U. contributed reagents and to the editing of the manuscript. L.B. and S.K. produced the vGATE viruses. M.T.H. and V.G. participated in the design of the vGATE-based experiment, the interpretation of the results, and the correction of the manuscript. A.D. participated in the design of the experiments, the interpretation of the results and literature, and the writing of the manuscript.

DECLARATION OF INTERESTS

The authors declare no competing interests.

Received: July 21, 2022
Revised: August 17, 2022
Accepted: August 19, 2022
Published: September 15, 2022

REFERENCES

1. Ellingsen, D.M., Leknes, S., Løseth, G., Wessberg, J., and Olausson, H. (2015). The neurobiology shaping affective touch: expectation, motivation, and meaning in the multisensory context. Front. Psychol. *6*, 1986. https://doi.org/10.3389/fpsyg.2015.01986.
2. Ebbesen, C.L., and Froemke, R.C. (2021). Body language signals for rodent social communication. Curr. Opin. Neurobiol. *68*, 91–106. https://doi.org/10.1016/j.conb.2021.01.008.
3. Zilkha, N., Sofer, Y., Kashash, Y., and Kimchi, T. (2021). The social network: neural control of sex differences in reproductive behaviors, motivation, and response to social isolation. Curr. Opin. Neurobiol. *68*, 137–151. https://doi.org/10.1016/j.conb.2021.03.005.
4. Ahmadlou, M., Houba, J.H.W., van Vierbergen, J.F.M., Giannouli, M., Gimenez, G.A., van Weeghel, C., Darbanfouladi, M., Shirazi, M.Y., Dziubek, J., Kacem, M., et al. (2021). A cell type-specific cortico-subcortical brain circuit for investigatory and novelty-seeking behavior. Science *372*, eabe9681. https://doi.org/10.1126/science.abe9681.
5. Kappel, J.M., Förster, D., Slangewal, K., Shainer, I., Svara, F., Donovan, J.C., Sherman, S., Januszewski, M., Baier, H., and Larsch, J. (2022). Visual recognition of social signals by a tectothalamic neural circuit. Nature *608*, 146–152. https://doi.org/10.1038/s41586-022-04925-5.
6. Tang, Y., Benusiglio, D., Lefevre, A., Hilfiger, L., Althammer, F., Bludau, A., Hagiwara, D., Baudon, A., Darbon, P., Schimmer, J., et al. (2020). Social touch promotes interfemale communication via activation of parvocellular oxytocin neurons. Nat. Neurosci. *23*, 1125–1137. https://doi.org/10.1038/s41593-020-0674-y.
7. Zelikowsky, M., Hui, M., Karigo, T., Choe, A., Yang, B., Blanco, M.R., Beadle, K., Gradinaru, V., Deverman, B.E., and Anderson, D.J. (2018). The neuropeptide Tac2 controls a distributed brain state induced by chronic social isolation stress. Cell *173*, 1265–1279.e19. https://doi.org/10.1016/j.cell.2018.03.037.
8. Usdin, T.B., Hoare, S.R., Wang, T., Mezey, E., and Kowalak, J.A. (1999). TIP39: a new neuropeptide and PTH2-receptor agonist from hypothalamus. Nat. Neurosci. *2*, 941–943.
9. Anneser, L., Alcantara, I.C., Gemmer, A., Mirkes, K., Ryu, S., and Schuman, E.M. (2020). The neuropeptide Pth2 dynamically senses others via mechanosensation. Nature *588*, 653–657. https://doi.org/10.1038/s41586-020-2988-z.
10. Cservenák, M., Szabó, E.R., Bodnár, I., Lékó, A., Palkovits, M., Nagy, G.M., Usdin, T.B., and Dobolyi, A. (2013). Thalamic neuropeptide mediating the effects of nursing on lactation and maternal motivation. Psychoneuroendocrinology *38*, 3070–3084. https://doi.org/10.1016/j.psyneuen.2013.09.004.
11. Dobolyi, A., Cservenák, M., and Young, L.J. (2018). Thalamic integration of social stimuli regulating parental behavior and the oxytocin system. Front. Neuroendocrinol. *51*, 102–115. https://doi.org/10.1016/j.yfrne.2018.05.002.
12. Cservenák, M., Keller, D., Kis, V., Fazekas, E.A., Öllös, H., Lékó, A.H., Szabó, E.R., Renner, É., Usdin, T.B., Palkovits, M., and Dobolyi, A. (2017). A thalamo-hypothalamic pathway that activates oxytocin neurons in social contexts in female rats. Endocrinology *158*, 335–348. https://doi.org/10.1210/en.2016-1645.
13. Dobolyi, A., Dimitrov, E., Palkovits, M., and Usdin, T.B. (2012). The neuroendocrine functions of the parathyroid hormone 2 receptor. Front. Endocrinol. (Lausanne) *3*, 121. https://doi.org/10.3389/fendo.2012.00121.
14. Hasan, M.T., Althammer, F., Silva da Gouveia, M., Goyon, S., Eliava, M., Lefevre, A., Kerspern, D., Schimmer, J., Raftogianni, A., Wahis, J., et al. (2019). A fear memory engram and its plasticity in the hypothalamic oxytocin system. Neuron *103*, 133–146.e8. https://doi.org/10.1016/j.neuron.2019.04.029.
15. Cservenák, M., Kis, V., Keller, D., Dimén, D., Menyhárt, L., Oláh, S., Szabó, E.R., Barna, J., Renner, É., Usdin, T.B., and Dobolyi, A. (2017). Maternally involved galanin neurons in the preoptic area of the rat. Brain Struct. Funct. *222*, 781–798. https://doi.org/10.1007/s00429-016-1246-5.
16. Paxinos, G., and Watson, C. (2007). The Rat Brain in Stereotaxic Coordinates (Academic Press).
17. Mai, J.K. (2008). Atlas of the Human Brain (Academic Press).
18. Cservenák, M., Bodnár, I., Usdin, T.B., Palkovits, M., Nagy, G.M., and Dobolyi, A. (2010). Tuberoinfundibular peptide of 39 residues is activated during lactation and participates in the suckling-induced prolactin release in rat. Endocrinology *151*, 5830–5840.
19. Fernandes, A.M., Beddows, E., Filippi, A., and Driever, W. (2013). Orthopedia transcription factor otpa and otpb paralogous genes function during dopaminergic and neuroendocrine cell specification in larval zebrafish. PLoS One *8*, e75002. https://doi.org/10.1371/journal.pone.0075002.
20. Dobolyi, A., Palkovits, M., and Usdin, T.B. (2010). The TIP39-PTH2 receptor system: unique peptidergic cell groups in the brainstem and their interactions with central regulatory mechanisms. Prog. Neurobiol. *90*, 29–59.
21. Nagalski, A., Puelles, L., Dabrowski, M., Wegierski, T., Kuznicki, J., and Wisniewska, M.B. (2016). Molecular anatomy of the thalamic complex and the underlying transcription factors. Brain Struct. Funct. *221*, 2493–2510. https://doi.org/10.1007/s00429-015-1052-5.
22. Dobolyi, A., Wang, J., Irwin, S., and Usdin, T.B. (2006). Postnatal development and gender-dependent expression of TIP39 in the rat brain. J. Comp. Neurol. *498*, 375–389.
23. Shamay-Tsoory, S.G., and Eisenberger, N.I. (2021). Getting in touch: a neural model of comforting touch. Neurosci. Biobehav. Rev. *130*, 263–273. https://doi.org/10.1016/j.neubiorev.2021.08.030.
24. Palkovits, M., Helfferich, F., Dobolyi, A., and Usdin, T.B. (2009). Acoustic stress activates tuberoinfundibular peptide of 39 residues neurons in the rat brain. Brain Struct. Funct. *214*, 15–23.
25. Dobolyi, A., Palkovits, M., Bodnár, I., and Usdin, T.B. (2003). Neurons containing tuberoinfundibular peptide of 39 residues project to limbic, endocrine, auditory and spinal areas in rat. Neuroscience *122*, 1093–1105.
26. Tsuneoka, Y., and Funato, H. (2021). Cellular composition of the preoptic area regulating sleep, parental, and sexual behavior. Front. Neurosci. *15*, 649159. https://doi.org/10.3389/fnins.2021.649159.
27. Ebert, D.H., and Greenberg, M.E. (2013). Activity-dependent neuronal signalling and autism spectrum disorder. Nature *493*, 327–337. https://doi.org/10.1038/nature11860.
28. Deschrijver, E., Wiersema, J.R., and Brass, M. (2017). Action-based touch observation in adults with high functioning autism: can compromised self-other distinction abilities link social and sensory everyday problems? Soc. Cogn. Affect. Neurosci. *12*, 273–282. https://doi.org/10.1093/scan/nsw126.

29. Krashes, M.J., Koda, S., Ye, C., Rogan, S.C., Adams, A.C., Cusher, D.S., Maratos-Flier, E., Roth, B.L., and Lowell, B.B. (2011). Rapid, reversible activation of AgRP neurons drives feeding behavior in mice. J. Clin. Invest. *121*, 1424–1428. https://doi.org/10.1172/JCI46229.

30. Fenno, L.E., Mattis, J., Ramakrishnan, C., Hyun, M., Lee, S.Y., He, M., Tucciarone, J., Selimbeyoglu, A., Berndt, A., Grosenick, L., et al. (2014). Targeting cells with single vectors using multiple-feature boolean logic. Nat. Methods *11*, 763–772. https://doi.org/10.1038/nmeth.2996.

31. Abràmoff, M.D., Magalhães, P.J., and Ram, S.J. (2004). Image processing with ImageJ. https://imagejnihgov/ij.

32. Péter, A. (2016). Solomon Coder: a simple solution for behavior coding. v 16.06.26. http://solomoncoder.com/.

33. Bankhead, P., Loughrey, M.B., Fernández, J.A., Dombrowski, Y., McArt, D.G., Dunne, P.D., McQuaid, S., Gray, R.T., Murray, L.J., Coleman, H.G., et al. (2017). QuPath: open source software for digital pathology image analysis. Sci. Rep. *7*, 16878. https://doi.org/10.1038/s41598-017-17204-5.

34. Dimén, D., Puska, G., Szendi, V., Sipos, E., Zelena, D., and Dobolyi, Á. (2021). Sex-specific parenting and depression evoked by preoptic inhibitory neurons. iScience *24*, 103090. https://doi.org/10.1016/j.isci.2021.103090.

35. Schweinfurth, M.K. (2020). The social life of Norway rats (Rattus norvegicus). eLife *9*, e54020. https://doi.org/10.7554/eLife.54020.

36. Dobolyi, A., Ueda, H., Uchida, H., Palkovits, M., and Usdin, T.B. (2002). Anatomical and physiological evidence for involvement of tuberoinfundibular peptide of 39 residues in nociception. Proc. Natl. Acad. Sci. USA *99*, 1651–1656.

37. Wang, J., Palkovits, M., Usdin, T.B., and Dobolyi, A. (2006). Forebrain projections of tuberoinfundibular peptide of 39 residues (TIP39)-containing subparafascicular neurons. Neuroscience *138*, 1245–1263.

38. Dobolyi, A. (2009). Central amylin expression and its induction in rat dams. J. Neurochem. *111*, 1490–1500.

39. McIlmoyl, M. (1965). Two neurological staining techniques utilizing the dye luxol fast blue. Can. J. Med. Technol. *27*, 118–123.

40. Wang, T., Palkovits, M., Rusnak, M., Mezey, E., and Usdin, T.B. (2000). Distribution of parathyroid hormone-2 receptor-like immunoreactivity and messenger RNA in the rat nervous system. Neuroscience *100*, 629–649.

41. Farkas, I., Kalló, I., Deli, L., Vida, B., Hrabovszky, E., Fekete, C., Moenter, S.M., Watanabe, M., and Liposits, Z. (2010). Retrograde endocannabinoid signaling reduces GABAergic synaptic transmission to gonadotropin-releasing hormone neurons. Endocrinology *151*, 5818–5829. https://doi.org/10.1210/en.2010-0638.

42. Kuo, J., and Usdin, T.B. (2007). Development of a rat parathyroid hormone 2 receptor antagonist. Peptides *28*, 887–892.

Please cite this article in press as: Keller et al., A thalamo-preoptic pathway promotes social grooming in rodents, Current Biology (2022), https://doi.org/10.1016/j.cub.2022.08.062

STAR★METHODS

KEY RESOURCES TABLE

REAGENT or RESOURCE	SOURCE	IDENTIFIER
Antibodies		
Mouse Anti-calbindin D-28k Antibody	Sigma Aldrich	Cat. #: C9848; RRID: AB_476894
Chicken Anti-mCherry Antibody	Abcam	Cat. #: AB205402; RRID: AB_2722769
Goat Anti-GFP Antibody	Abcam	Cat. #: AB5450; RRID: AB_304897
Mouse Anti-NeuN Antibody	Merck Millipore	Cat. #: MAB377; RRID: AB_2298767
Mouse Anti-Parvalbumin Antibody	Sigma Aldrich	Cat. #: P3088; RRID: 477329
Rabbit Anti-PTH2R Antibody	Gift from Ted B. Usdin	RRID: AB_2315229
Rabbit Anti-PTH2 Antibody	Gift from Ted B. Usdin	RRID: AB_2315466
Rabbit c-Fos Antibody	Santa Cruz Biotechnology	Cat. #: SC-166940; RRID: AB_10609634
Alexa Fluor 594 AffiniPure Donkey Anti-Rabbit IgG	Jackson ImmunoResearch	Cat. #: 711-585-152; RRID: AB_2340621
Alexa Fluor 594 AffiniPure Donkey Anti-Chicken IgY	Jackson ImmunoResearch	Cat. #: 703-585-155; RRID: AB_2340377
Alexa Fluor 594 AffiniPure Donkey Anti-Mouse IgG	Jackson ImmunoResearch	Cat. #: 715-585-150; RRID: AB_2340854
Cy5 AffiniPure Donkey Anti-Mouse IgG	Jackson ImmunoResearch	Cat. #: 715-175-151; RRID: AB_2340820
Biotin-SP (long spacer) AffiniPure Donkey Anti-Chicken IgY (IgG)	Jackson ImmunoResearch	Cat. #: 703-065-155; RRID: AB_2313596
Biotin-SP (long spacer) AffiniPure Donkey Anti-Goat IgY (IgG)	Jackson ImmunoResearch	Cat. #: 705-065-003; RRID: AB_ 2340396
Biotin-SP (long spacer) AffiniPure Donkey Anti-Mouse IgY (IgG)	Jackson ImmunoResearch	Cat. #: 715-065-150; RRID: AB_ 2307438
Biotin-SP (long spacer) AffiniPure Donkey Anti-Rabbit IgY (IgG)	Jackson ImmunoResearch	Cat. #: 711-065-152; RRID: AB_ 2340593
Bacterial and virus strains		
pAAV-hSyn-hM3D(Gq)-mCherry	Bryan Roth	Addgene; 50474-AAV5
pAAV-hSyn-hM4D(Gi)-mCherry	Bryan Roth	Addgene; 50475-AAV5
pAAV-hSyn-mCherry	Karl Deisseroth	Addgene; 114472-AAV5
pAAV-hSyn-DIO-hM3D(Gq)-mCherry	Bryan Roth[29]	Addgene; 44361-AAV5
pAAV-hSyn-DIO-hM4D(Gi)-mCherry	Bryan Roth	Addgene; 44362-AAV5
pAAV-hSyn-DIO-mCherry	Bryan Roth	Addgene; 50459-AAV5
AAVrg-Ef1a-mCherry-IRES-Cre	Karl Deisseroth[30]	Addgene; 55632-AAVrg
pAAV-hSyn-DIO-HA-hM3D(Gq)-IRES-mCitrine	Bryan Roth	Addgene; 50454-AAV8
pAAV-hSyn-DIO-HA-hM4D(Gi)-IRES-mCitrine	Bryan Roth	Addgene; 50455-AAV8
rAAV-$(tetO)_7$-$\mathbf{P}_{fos}$-rtTA	Gift from Valery Grinevich[14]	N/A
rAAV-$\mathbf{P}_{tet}$bi-Cre/YC3.60	Gift from Valery Grinevich[14]	N/A
Experimental models: Organisms/strains		
Rat: wild type	Wistar	N/A
Mouse: PTH2R-Cre	Ted B. Usdin, NIH	N/A
Mouse: VGAT-IRES-Cre knock-in mice (*Slc32a1*$^{tm2(cre)Lowl}$/J)	The Jackson Laboratory	Stock No: 016962
Mouse: Ai6(RCL-ZsGreen (B6.Cg-*Gt(ROSA)26Sor*$^{tm6(CAG-ZsGreen1)Hze}$/J)	The Jackson Laboratory	Stock No: 007906

(*Continued on next page*)

Please cite this article in press as: Keller et al., A thalamo-preoptic pathway promotes social grooming in rodents, Current Biology (2022), https://doi.org/10.1016/j.cub.2022.08.062

Continued

REAGENT or RESOURCE	SOURCE	IDENTIFIER
Software and algorithms		
ImageJ	Image Processing with ImageJ[31]	https://imagej.nih.gov/ij
Solomon Coder	Solomon Coder (Version Beta: 17.03.22)[32]	https://solomon.andraspeter.com
QuPath	Bankhead et al.[33]	https://qupath.github.io
SMART Video Tracking software	Panlab Harvard Apparatus	https://www.panlab.com/en/products/smart-video-tracking-software-panlab
Other		
PTH2R antagonist	Bio-Kasztel Kft., Hungary	Cat. # NBL
VECTASTAIN Elite ABC-HRP Kit, Peroxidase	Vector Laboratories, Burlingame, CA, USA	Cat. # PK-6100
DAB Substrate Kit, Peroxidase (HRP), with Nickel, (3,3'-diaminobenzidine)	Vector Laboratories, Burlingame, CA, USA	Cat. # SK-4100
Aqua-Poly/Mount	VWR	Cat. # 87001-902
DePeX mounting medium	Sigma Aldrich	Cat. # 06522

RESOURCE AVAILABILITY

Lead contact

Further information and requests for resources and reagents should be directed to and will be fulfilled by the lead contact, Arpad Dobolyi (dobolyi.arpad@ttk.elte.hu).

Materials availability

This study did not generate new unique reagents.

Data and code availability

- Single-cell RNA-seq data and Western blot images have not been generated in the present study. Microscopy data reported in this paper will be shared by the lead contact upon request.
- No original code was used in the analysis of the data.
- Any additional information required to reanalyze the data reported in this paper is available from the lead contact upon request.

EXPERIMENTAL MODEL AND SUBJECT DETAILS

Animals

The Workplace Animal Welfare Committee of the National Scientific Ethical Committee on Animal Experimentation at Semmelweis and Eötvös Loránd Universities, Budapest, specifically approved this study (PE/EA/926-7/2021 and PE/EA/568-7/2020, respectively). Thus, the procedures involving rats and mice were carried out according to experimental protocols that meet the guidelines of the Animal Hygiene and Food Control Department, Ministry of Agriculture, Hungary (40/2013), which is in accordance with EU Directive 2010/63/EU for animal experiments. A total of 174 adult rats (Wistar; Charles Rivers Laboratories, Hungary) were used (7 females and 8 males for chemogenetic stimulation of the PIL, 10 females and 9 males for chemogenetic inhibition of the PIL, 8 females and 5 males for control virus, 3 for viral injection into the SN, 10 for anterograde tracer injection into the PIL and SN, 15 for social c-Fos study, 12 for chemogenetics / c-Fos study, 9 for vGATE PIL stimulation, 8 for vGATE PIL inhibition, 6 for vGATE control virus, 6 for vGATE protocol control, 12 for double injections into the PIL and MPOA, 6 for cannula implantation into the MPOA for CNO administration, 2 for labeling with PTH2 in MPOA, 13 for osmotic minipump study, 5 for labeling with PTH2 with calbindin and parvalbumin, 20 for qRT-PCR study). In the behavioral experiments, vaginal smear tests were used to select diestrous rats for the testing. All of the rats were 90-120 days old when sacrificed. A total of 14 adult female mice were used in the study. There were 8 PTH2R-ZsGreen mice (offspring of PTH2R-Cre (generated by Ted B. Usdin, NIH) and GtROSA26Sor_CAG/ZsGreen1 mice (The Jackson Laboratory; stock number: 007906)) for labeling PTH2R and c-Fos, 3 VGAT-ZsGreen mice (offspring of VGAT-IRES-Cre and GtROSA26Sor_CAG/ZsGreen1 mice (The Jackson Laboratory; stock numbers: 016962 and 007906)) for labeling with VGAT and c-Fos/PTH2, 3 VGAT-ZsGreen mice for patch-clamp experiment. There were no behavioral or health issues found in VGAT-Cre and PTH2R-Cre mice crossed with reporter mice as we described previously.[34] All of the mice were 100-150 days old when sacrificed. Animals were kept under standard laboratory conditions with 12-h light, 12-h dark periods (lights on at 6.00 a.m.), and supplied with food and drinking water *ad libitum*. Animals were anaesthetized with an intramuscular injection of anesthetic mix containing 0.4 ml/300g body weight ketamine (50 mg/ml) and 0.2 ml/300g body weight xylazine (20 mg/ml) for surgery, perfusions and dissections.

Please cite this article in press as: Keller et al., A thalamo-preoptic pathway promotes social grooming in rodents, Current Biology (2022), https://doi.org/10.1016/j.cub.2022.08.062

Viral vectors

PIL stimulation or silencing was performed with the following viruses: rAAV-**P**$_{hSYN}$-hM3D(Gq)-mCherry (Addgene plasmid # 50474; http://n2t.net/addgene:50474; RRID: Addgene_50474) and rAAV-**P**$_{hSYN}$-hM4D(Gi)-mCherry (Addgene plasmid # 50475; http://n2t.net/addgene:50475; RRID: Addgene_50475), which were gifts from Bryan Roth. rAAV-**P**$_{hSYN}$-mCherry, used as control virus, was a gift from Karl Deisseroth (Addgene plasmid # 114472; http://n2t.net/addgene:114472; RRID: Addgene_114472).

Activity-dependent tagging of PIL neurons was performed with a virus cocktail, which included the following viruses: 1. rAAV-(tetO)$_7$-**P**$_{fos}$-rtTA; 2. rAAV-**P**$_{tet}$bi-Cre/YC3.60; 3. rAAV-**P**$_{hSYN}$-DIO-hM3D(Gq)-mCherry (a gift from Bryan Roth, Addgene plasmid # 44361; http://n2t.net/addgene:44361; RRID: Addgene_44361[29] or rAAV-**P**$_{hSYN}$-DIO-hM4D(Gi)-mCherry (a gift from Bryan Roth, Addgene plasmid # 50475; http://n2t.net/addgene:50475; RRID: Addgene_50475) or rAAV-**P**$_{hSYN}$-DIO-mCherry (a gift from Bryan Roth, Addgene plasmid # 50459; http://n2t.net/addgene:50459; RRID: Addgene_50459), the first 2 viruses were the same as used in our previous study, Hasan et al.[14].

For chemogenetic activation of PIL neurons projecting to the MPOA, first, a retrogradely spreading virus (AAVrg-Ef1a-mCherry-IRES-Cre, which was a gift from Karl Deisseroth (Addgene plasmid # 55632; http://n2t.net/addgene:55632; RRID: Addgene_55632))[30] was targeted to both sides of the MPOA. Then, three weeks later, a second virus (rAAV-**P**$_{hSYN}$-DIO-HA-hM3D(Gq)-IRES-mCitrine, Addgene plasmid # 50454; http://n2t.net/addgene:50454; RRID: Addgene_50454; or rAAV-**P**$_{hSYN}$-DIO-HA-hM4D(Gi)-IRES-mCitrine, Addgene plasmid # 50455; http://n2t.net/addgene:50455; RRID:Addgene_50455) was injected into the PIL in both sides, which were gifts from Bryan Roth.

METHOD DETAILS

Histology

Animal brain tissue collection and sectioning

Animals were deeply anesthetized and perfused transcardially with 150 ml of saline followed by 300 ml of ice-cold 4% paraformaldehyde (PFA) prepared in 0.1 M phosphate buffer at pH = 7.4 (PB) for rats and with 15 ml of saline followed by 30 ml of ice-cold 4% PFA prepared in 0.1 M PB for mice. Brains were removed and postfixed in 4% PFA for 24 h, and then transferred to PB containing 20% sucrose for 2 days. Serial coronal sections were cut at 40 μm on a sliding microtome and sections were collected in PB containing 0.05% sodium-azide and stored at 4 °C.

Immunolabeling

Every fifth free-floating brain section in rats and every third in mice were used for each labeling. First, the sections were pretreated in PB containing 0.3% hydrogen peroxide (H_2O_2) for 15 min to eliminate endogenous peroxidase activity, then in PB containing 0.5% Triton X-100 and 3% bovine serum albumin for 1 h for antibody penetration and reduction of nonspecific labeling, respectively. Then, primary antisera (Table S3) were applied for 24 h at room temperature. This was followed by incubation of the sections in biotinylated or fluorescent secondary antibodies (Jackson ImmunoResearch, Table S3) for 1 h. For non-fluorescent single labeling and for tyramide amplification fluorescent labeling, the sections were incubated in avidin-biotin-peroxidase complex (ABC, 1:500; Vector Laboratories) for 1 h. Subsequently, sections were treated with 0.02% 3,3'-diaminobenzidine (DAB; Vector Laboratories), 0.08% nickel (II) sulfate and 0.003% H_2O_2 in Tris hydrochloride buffer (0.1 M, pH = 8.0) for 6 min for non-fluorescent immunoperoxidase technique, and with FITC-tyramide (1:5,000) and H_2O_2 for tyramide amplification immunofluorescence. For double labeling, another primary antibody (Table S3), produced in a different species as the first antibody, was added at room temperature overnight. Sections were incubated in secondary antibodies produced in donkey and labeled with Alexa dyes (1:500; Jackson ImmunoResearch) for 2 h. Finally, the sections were mounted, dehydrated and coverslipped with DePeX Mounting Medium (Sigma) for non-fluorescent, and Aqua-Poly/Mount (VWR) for fluorescent labeling.

Anterograde tracing with biotinylated dextran amine

Injection of anterograde tracer into the PIL

The anterograde tracer biotinylated dextran amine (BDA, 10,000 MW; Molecular Probes) was targeted to the PIL (n = 5). Some of the misplaced injections were used as controls (n = 5). For stereotaxic injections, rats were positioned in a stereotaxic apparatus with the incisor bar set at -3.3 mm. Holes of about 1 mm diameter were drilled into the skull above the target coordinates. Glass micropipettes of 15–20 μm internal diameter were filled with 10% BDA dissolved in PB and lowered to the following stereotaxic coordinates[16]: AP = −5.2 mm from bregma, ML = +2.6 mm from the midline, DV = −6.8 mm from the surface of the dura mater. Once the pipette was in place, the BDA was injected by iontophoresis by using a constant current source (51413 Precision Current Source, Stoelting, Wood Dale, IL) that delivered a current of +6 μA, which pulsed for 7 sec on and 7 sec off for 15 min. Then the pipette was left in place for 10 min with no current and withdrawn under negative current. After tracer injections, the animals were allowed to survive for 7 days. Visualization of BDA was done as described above for Ni-DAB visualization.

Social c-Fos activation study

Social interaction experiment

Female rat littermates (n = 15) kept together (housed 2 per cage) were used in the study. The 2 rats were isolated for 22 h to reduce basal c-Fos activation. Then, the rats were reunited again in the cage they had cohabited. 7 rats could freely interact with their cagemate while 4 rats were isolated from their partner with bars, so they could see, hear and smell each other but could not directly

Please cite this article in press as: Keller et al., A thalamo-preoptic pathway promotes social grooming in rodents, Current Biology (2022), https://doi.org/10.1016/j.cub.2022.08.062

interact. Control females (n = 4) continued to be kept isolated. All animals were sacrificed 24 h after the beginning of isolation, i.e. 2 h after reunion of the socially interacting group. Animals were perfused transcardially as described above, and processed for c-Fos immunohistochemistry.

c-Fos immunohistochemistry

The procedure was performed as described above for immunolabeling using rabbit anti-c-Fos primary antiserum (1:3000; Santa Cruz Biotechnology) and Ni-DAB visualization.

Analysis of c-Fos immunolabeling

The sections containing the greatest number of c-Fos-ir neurons in the investigated brain regions (ILC, LS, MPOA, PVN, MeA, DMH, VLPAG) were selected from each of the 15 animals, and an image was taken of them using 10x objective. The total number of c-Fos-ir neurons in the selected brain area was counted using ImageJ 1.53e program[31] as described previously.[12] Briefly, the same algorithm, based on intensity, size, and circularity thresholding was used for all images to select the Fos-ir nuclei, whose number was counted automatically by the program. Spots were selected whose brightness intensity value was <150. The number of c-Fos–containing cells was defined as the number of selected spots counted in a size ranging from 20 to 100 pixels, and a circularity factor between 0.5 and 1.0. Statistical analyses were performed using Prism 9 for Windows (GraphPad Software, La Jolla, CA). The number of c-Fos-ir neurons in the 3 groups (after social interaction, social interaction without direct contact, isolated control) was compared using one-way ANOVA.

Viral vector-based chemogenetics

Chemogenetic activation or silencing of the PIL

rAAV-$\mathbf{P}_{hSYN}$-hM3D(Gq)-mCherry; rAAV-$\mathbf{P}_{hSYN}$-hM4D(Gi)-mCherry or rAAV-$\mathbf{P}_{hSYN}$-mCherry was injected to the PIL (female rats: n = 7 for stimulation, n = 10 for inhibition and n = 8 for control virus; male rats: n = 8 for stimulation, n = 9 for inhibition and n = 5 for control virus). Some of the misplaced injections were used as controls in tract tracing (n = 3). For stereotaxic injections, rats were positioned in a stereotaxic apparatus with the incisor bar set at -3.3 mm. Holes of about 1 mm diameter were drilled into the skull above the target coordinates. A Hamilton pipette (volume 1 μl) was filled with the solution containing the virus and lowered to the following stereotaxic coordinates[16]: AP = −5.2 mm from bregma, ML = ±2.6 mm from the midline, DV = −6.8 mm from the surface of the dura mater. Once the pipette was in place, 100 nl virus was pressure injected into the PIL (10 nl/min), then the pipette was left in place for 10 min. Following the slow withdrawal of the pipette, we repeated the same protocol on the other side of the brain. After the injections, the animals were isolated for two weeks for recovery, then they were reunited with their familiar cagemate for one week before the behavior tests took place.

Activity-dependent tagging: Chemogenetic manipulation of PIL neurons activated upon social encounter The protocol for bilateral injections of the vGATE viral cocktail into the PIL was as described above. The viral cocktail included the following viruses: 1. rAAV-(tetO)7-Pfos-rtTA; 2. rAAV-Ptetbi-Cre/YC3.60; 3. rAAV-PhSYN-DIO-hM3D(Gq)-mCherry (excitatory, n = 9), or rAAV-$\mathbf{P}_{hSYN}$-DIO-hM4D(Gi)-mCherry (inhibitory, n = 8) or rAAV-$\mathbf{P}_{hSYN}$-DIO-mCherry (control, n = 8). 600 nl of single injection contained the following: 1st virus: 225 nl. 2nd virus: 75 nl, 3rd virus: 300 nl (3/1/4 ratio). After two weeks of recovery, the animals were treated with i.p. doxycycline hyclate injection (5 mg/kg body weight (bw) dissolved in the mixture of 0.01M PB and 0.9% NaCl, 2 : 1 ratio), then, the following day, they were reunited with one of their cagemates for 2 hours for expression of DREADD in neurons that are c-Fos-positive in the PIL in response to social interaction. The behavior tests started 10 days later.

Chemogenetic manipulation of PIL neurons projecting to the MPOA

First, a retrogradely spreading virus (AAVrg-Ef1a-mCherry-IRES-Cre) was targeted to both sides of the MPOA. Then, three weeks later, a second virus (rAAV-$\mathbf{P}_{hSYN}$-DIO-HA-hM3D(Gq)-IRES-mCitrine or rAAV-$\mathbf{P}_{hSYN}$-DIO-HA-hM4D(Gi)-IRES-mCitrine) was injected into the PIL in both sides (n = 6 for each group). The viral injections were carried out as described above. The stereotaxic coordinates of the MPOA was the following[16]: AP = −0.5 mm from bregma, ML = ±0.6 mm from the midline, DV = −6.7 and −7.7 mm from the surface of the dura mater. The MPOA was targeted in two ventral coordinates, 100 nl of virus was injected at both levels.

Chemogenetic activation of axonal terminals of PIL neurons in the MPOA

Implantation of cannulae into the MPOA was performed immediately after the injection of the excitatory virus (rAAV-$\mathbf{P}_{hSYN}$-hM3D(Gq)-mCherry, see above) as described above. In rats (n = 6) already anaesthetized with 0.2 ml xylazine and 0.4 ml ketamine and fixed in a stereotaxic apparatus, a hole of about 1 mm diameter was drilled into the skull above at the following coordinates[16]: AP = −0.5 mm from bregma, ML = ±3.0 mm from the midline. Cannulae (ALZET Brain Infusion Kit 2, Durect) were inserted into the MPOA (V = 7.2 mm) with an inclination angle of 16.5° and fixed to the skull with cranioplastic cement. Subsequently, the same protocol was repeated on the other side. After the operation, Tardomyocel comp. III antibiotics (0.1 ml/kg bw) was given s.c. to the animals for 5 days to prevent infections.

Osmotic minipump

For the direct and sustained infusion of PTH2R antagonist, HYWH-TIP39 into the lateral ventricle, we used Alzet Osmotic minpump, Durect (0.5 μl/h, 14 days, 0.3 ml) combined with Alzet Brain Infusion Kit 2, Durect with two spacers attached (4.0 mm depth of cannula tube). In rats (n = 13) anaesthetized with 0.2 ml xylazine and 0.4 ml ketamine and fixed in a stereotaxic apparatus, a hole of about 1 mm diameter was drilled into the skull above at the following coordinates[16]: AP = −0.5 mm from bregma, ML = +1.6 mm from the midline. Cannula (ALZET Brain Infusion Kit 2, Durect) was inserted into the LV (V = 4.0 mm) and fixed to the skull with cranioplastic cement. The osmotic minipump was placed at the back of the animal subcutaneously and was filled with ACSF (n = 7) or PTH2 receptor antagonist

Please cite this article in press as: Keller et al., A thalamo-preoptic pathway promotes social grooming in rodents, Current Biology (2022), https://doi.org/10.1016/j.cub.2022.08.062

(n = 6). The PTH2R antagonist HYWH-PTH2 (sequence: SLAHYWHAAFRERARLLAALERRHWLNSYMHKLLVLDAP, Bio-Kasztel Kft., Hungary) was dissolved in ACSF (1.5 mg/ml; administered 18 μg/day with the speed of 0.5 μl/h).

Social behavioral tests

Clozapine-N-oxide (CNO) injection

In case of the viral vector-based chemogenetics, 1.5 h before the behavioral experiments, the animals were isolated from their cagemates, which was followed by the intraperitoneal administration of CNO or vehicle. On the first day of the experimental session, control vehicle injection (5% dimethyl sulfoxide (DMSO)dissolved in distilled water, 1 ml/kg bw) was used. One day later, CNO was administered i.p. (0.3 mg/kg bw CNO, dissolved in 5% DMSO dissolved in distilled water, 1 ml/kg bw). This was followed by another control injection three days later.

Freely moving social behavior test

The animals were habituated to the open field arena (40 x 80 cm) one day before the experiment. On the experimental day, the animals were placed in the open field arena where the subject and the stimulus rat could freely interact with each other and 10 minutes of footage was recorded. The following social behavior elements were distinguished[6,35]: anogenital sniffing (“one individual sniffs or licks the anogenital region of a conspecific”), non-anogenital sniffing (“one individual shows enhanced sniffing at colony members”), chasing (“one individual runs after a second”), social grooming (“one individual gently nibbles or licks the fur of a conspecific, sometimes with the aid of its forepaws”, mounting (“walks over a conspecific, that is typically the more dominant”, and passive social interaction (one gets into contact with conspecific without performing one of the above mentioned behavior elements, e. g. side-to-side contact).

The duration of the different types of performed behaviors were measured by using Solomon Coder[32] software (https://solomon.andraspeter.com/). The duration of the behavioral elements was compared between the groups using repeated measures ANOVA followed by Šídák’s multiple comparisons tests.

Social interaction test without direct contact

In another experiment, direct contact between the animals was not allowed. Instead, the stimulus rat was placed in a small cage with wall made of bars, so they could just smell, hear and see each other while 10 min of footage was recorded.

The behavior of the animals in the experiment excluding the physical contact was analyzed with SMART Video Tracking software v3.0 (Panlab Harvard Apparatus). The duration of social interaction without direct contact (when the experimental rat approached the small cage within 5 cm) was compared between the groups using one-way ANOVA followed by Šídák’s multiple comparisons tests.

Social novelty test

The experiment measuring the preference for social novelty was conducted in the Three Chambers Sociability Apparatus (120 x 80 cm, including three 40 x 80 cm chambers connected with doors). The animals were habituated to the apparatus one day before the experiment. On the experimental day, 1.5 hour after the administration of drug (control or CNO injection, see above), the subject was placed in the middle chamber. Each side chamber contained a small cage with wall made of bars, in one of them the familiar cagemate of the subject, in the other one an unfamiliar animal were placed. During the 10 min of the experiment, the subject could freely move between the three chambers. The behavior of the animal was analyzed with SMART Video Tracking software v3.0 (Panlab Harvard Apparatus). The duration of the time spent in the chambers was compared between the groups using two-tailed paired t tests.

Induction of c-Fos expression driven by chemogenetic stimulation

Female rats (n = 12) were injected with excitatory virus (rAAV-$\mathbf{P}_{hSYN}$-hM3D(Gq)-mCherry) into the PIL as described above. Three weeks later, 6 animals received control i.p. injection (5% DMSO dissolved in distilled water, 1 ml/kg bw) and 6 animals were injected i.p. with CNO (0.3 mg/kg bw CNO, dissolved in 5% DMSO dissolved in distilled water, 1 ml/kg bw). All animals were sacrificed 2 h after the drug administration. Animals were perfused transcardially and processed for c-Fos immunohistochemistry as described above. The sections containing the greatest number of c-Fos-ir neurons in the investigated brain regions (PIL, ILC, LS, MPOA, PVN, MeA, DMH, VLPAG) were selected from each of the 12 animals and analyzed as described above for social c-Fos study. The number of c-Fos-ir neurons in the two groups was compared using two-way ANOVA followed by Šídák’s multiple comparisons tests.

Immunohistochemical characterisation of neurons in the PIL→MPOA pathway

Single labeling of mCherry

The injection sites of viruses as well as the projection pattern of the infected neurons was studied using immunoperoxidase technique with the visualization of mCherry, for which a chicken anti-mCherry antiserum (1:1,000; Abcam) was used with Ni-DAB method.

The rats, in which over 80% of the virally infected cells were located within the PIL, were only included in the behavioral analysis. For neuronal tract-tracing, the inclusion of animals was even more stringent as animals with infected neurons outside the PIL were not included in the analysis because adjacent brain regions do have distinct projection pattern.

Double labeling of mCherry with c-Fos, calbindin, parvalbumin and mCitrine

First, rabbit anti-c-Fos primary antiserum (1:750; Santa Cruz Biotechnology) or mouse anti-calbindin D-28k antiserum (1:1,500; Sigma) or mouse anti-parvalbumin antiserum (1:2,500; Sigma) or goat anti-GFP antiserum (1:1,000; Abcam) for mCitrine labeling was applied for 24 h at room temperature. This was followed by incubation of the sections in biotinylated donkey

Please cite this article in press as: Keller et al., A thalamo-preoptic pathway promotes social grooming in rodents, Current Biology (2022), https://doi.org/10.1016/j.cub.2022.08.062

anti-rabbit/mouse/goat secondary antibodies (1:1,000; Jackson ImmunoResearch). Subsequently, sections were treated with FITC-tyramide (1:5,000) and H_2O_2 in Tris hydrochloride buffer (0.1 M, pH = 8.0) for 6 min. Then, chicken anti-mCherry antiserum (1:1,000; Abcam) was applied at room temperature overnight. Following application of the primary antiserum, sections were incubated in donkey Alexa Fluor 594 anti-chicken secondary antibody (1:500; Jackson ImmunoResearch) for 2 h.

Triple labeling of c-Fos, PTH2 and NeuN

To visualize the neuronal activation upon social encounter in the MPOA, the animals (n = 4) kept in pairs were isolated for 22 h to reduce basal c-Fos activation. Then, the rats were reunited again in the cage they had cohabited for 2 h. Animals were perfused transcardially as described above, and processed for immunohistochemistry. First, rabbit anti-PTH2 primary antiserum (1:3,000) was applied and visualized with FITC-tyramide. Then, rabbit anti-c-Fos primary antiserum (1:750; Santa Cruz Biotechnology) was applied and visualized with donkey Alexa Fluor 594 anti-rabbit secondary antibody (1:500; Jackson ImmunoResearch) for 2 h. Finally, mouse anti-NeuN primary antiserum (1:500; Merck Millipore) was applied at room temperature overnight. Following the application of the primary antiserum, sections were incubated in donkey Cy5 anti-mouse secondary antibody (1:300; Jackson ImmunoResearch) for 2 h.

Labeling of c-Fos in PTH2R-ZsGreen mice

To visualize the neuronal activation of PTH2R-positive neurons upon social encounter in the MPOA, social c-Fos study was conducted as described above in PTH2R-ZsGreen mice (n = 4 for social group, n = 4 for isolated control). Then, the brains were processed for c-Fos immunohistochemistry as described above using visualization with Alexa Fluor 594. Then, 4′,6-diamidino-2-phenylindole (DAPI, 1:10,000) was applied at room temperature for 5 min.

Labeling of c-Fos/PTH2 in VGAT-ZsGreen mice

To visualize the neuronal activation of VGAT-positive neurons upon social encounter in the MPOA, a social c-Fos study was conducted in VGAT-ZsGreen mice as described above. The sections were processed for c-Fos and PTH2 immunolabeling using rabbit anti-c-Fos (1:500; Santa Cruz Biotechnology) or rabbit anti-PTH2 primary antisera (1:3,000).

Double labeling of PTH2 with calbindin or parvalbumin

Every fifth free-floating brain section was immunolabeled with tyramide amplification fluorescent immunolabeling using an affinity-purified anti-PTH2 antiserum (1:3,000) validated previously.[36,37] Then, mouse anti-calbindin D-28k (1:1,500; Sigma) or mouse anti-parvalbumin antiserum (1:2,500; Sigma) was applied at room temperature overnight. Following the application of the primary antiserum, sections were incubated in donkey Alexa Fluor 594 anti-mouse secondary antibody (1:500; Jackson ImmunoResearch) for 2 h.

Microdissection of brain tissue samples

For qRT-PCR, brains were dissected from 10 female adult rats kept in social environment (3 animals/cage) and 10 female adults isolated for two weeks prior to dissection. Immediately after the dissections of the brain, the PIL was microdissected as described previously in mother rats.[18] 1 mm thick coronal brain sections were cut from the freshly dissected brains. The area containing the PIL was subsequently microdissected from the appropriate coronal section with a circular micropunch needle of 1 mm diameter. The dissected tissue samples were quickly frozen in Eppendorf tubes on dry ice, and stored at -80°C until further processing.

Real-time PCR

Real-time qRT-PCR was carried out as described previously.[38] Briefly, total RNA was isolated from frozen PIL tissue samples using TRIzol reagent (Invitrogen, Carlsbad, CA, USA) as lysis buffer combined with RNeasy Mini kit (Qiagen, Germany) following the manufacturer's instructions. The concentration of RNA was adjusted to 500 ng/μL, and it was treated with Amplification Grade DNase I (Invitrogen). Then, cDNA was synthesized using SuperscriptII (Invitrogen) as described in the kit protocol. The cDNA was subsequently diluted (10x), and 2.5 μL of the resulting cDNA was used as template in multiplex PCR performed in duplicates using dual-fluorescence labeled TaqMan probes for *PTH2* (GenBank Accession Number (Rattus norvegicus): NM_001109144.1; 6-FAM-CGCTAGCTGACGACGCGGCCT-TAMRA), and glyceraldehyde-3-phosphatedehydrogenase (*GAPDH*; GenBank Accession Number (Rattus norvegicus): NM_017008.4; JOE-ATGGCCTTCCGTGTTCCTACCCCC-TAMRA) as the housekeeping gene as described previously.[18] The primers for *PTH2* (CTGCCTCAGGTGTTGCCCT and TGTAAGAGTCCAGCCAGCGG) were used at 300 nM, whereas the primers for *GAPDH* (CTGAACGGGAAGCTCACTGG and GGCATGTCAGATCCACAAC) were used at 150 nM concentration. The PCR reactions were performed with iTaq DNA polymerase (Bio-Rad Laboratories, Hercules, CA, USA) in total volumes of 12.5 μl under the following conditions: 95°C for 3 min, followed by 35 cycles of 95°C for 0.5 min, 60°C for 0.5 min, and 72°C for 1 min. Cycle threshold (Ct) values were obtained from the linear region of baseline adjusted amplification curves and duplicates were averaged. The data were expressed as the ratio of the housekeeping gene GAPDH using the following formula: log(Ct(GAPDH)-Ct(PTH2)). Statistical analyses were performed by unpaired t test for comparisons of the two groups.

Histology in the human brain

Human brain tissue samples

Human brain (n = 2) samples were collected in accordance with the Ethical Rules for Using Human Tissues for Medical Research in Hungary (HM 34/1999) and the Code of Ethics of the World Medical Association (Declaration of Helsinki). Tissue samples were taken during brain autopsy at the Department of Forensic Medicine of Semmelweis University in the framework of the Human Brain Tissue Bank (HBTB), Budapest. The activity of the HBTB has been authorized by the Committee of Science and Research Ethic of the Ministry of Health Hungary (ETT TUKEB: 189/KO/02.6008/2002/ETT) and the Semmelweis University Regional Committee of Science

Please cite this article in press as: Keller et al., A thalamo-preoptic pathway promotes social grooming in rodents, Current Biology (2022), https://doi.org/10.1016/j.cub.2022.08.062

and Research Ethic (No. 32/1992/TUKEB), including removal, collecting, storing and international transportation of human brain tissue samples and applying them for research. Prior written informed consent was obtained from the next of kin, which included the request to consult the medical chart and to conduct neurochemical analyses. The study reported in the manuscript was performed according to protocol approved by the Committee of Science and Research Ethics, Semmelweis University (TUKEB 189/2015). The medical history of the subjects (62 and 79 years old females died in sepsis and myocardial infarction, respectively) was obtained from clinical records, interviews with family members and relatives, as well as from pathological and neuropathological reports. All personal identifiers had been removed and samples were coded before the analyses of tissue. Brains were dissected from the skull with a *post-mortem* delay of 24-48 h. Brains were cut into 5–10 mm thick coronal slices and immersion fixed in 4% PFA in 0.1 M PB for 6–10 days.

For histological labeling, coronally oriented tissue blocks of about 10x10x20 mm containing the preoptic area and the PIL, respectively, were sectioned in the coronal plane. Tissue blocks containing the preoptic area (from 1 mm rostral to the anterior commissure to the caudal end of the preoptic area) and the posterior thalamic region containing the PIL were sectioned. Two days before sectioning, the tissue blocks were transferred to PB for 2 days to remove the excess PFA. Subsequently, the blocks were placed in PB containing 20% sucrose for 3 days for cryoprotection. Then, the blocks were frozen, and cut into 50 μm thick serial coronal sections on a sliding microtome.

Histological labeling in human brain sections

For cresyl-violet staining, sections were mounted consecutively on gelatin-coated slides and dried. Sections were stained in 0.1% cresyl-violet dissolved in PB and then differentiated in 96% ethanol containing acetic acid.

For Luxol fast blue staining, myelinated fibers were visualized first with the sulphonated copper phthalocyanine Luxol Fast Blue with a modification of the Kluver–Barrera method as described before.[39] Briefly, the sections were stained in 0.1% Luxol fast blue dissolved in 96% ethanol containing 0.05% acetic acid, and differentiated in 0.05% lithium-chloride followed by 70% ethanol. Subsequently, sections were stained in 0.1% cresyl-violet. At the end, sections were dehydrated and coverslipped as described above.

Immunolabeling in human brain sections

Immunolabeling was performed as described above on every 10th section. The free-floating sections were pretreated with 3% bovine serum albumin in PB containing 0.5% Triton X-100 for 30 min at room temperature. The sections were then placed in rabbit anti-PTH2R (1:20,000), mouse anti-calbindin D-28k (1:3,000; Sigma) or mouse anti-parvalbumin (1:5,000; Sigma) primary antiserum for 48 h at room temperature. The custom made anti-PTH2R antiserum was previously used and characterized.[40] Following the incubation in primary antisera, the sections were placed in biotinylated anti-rabbit/mouse secondary antibody (1:600; Vector Laboratories) for 2 h followed by incubation in a solution containing avidin–biotin–peroxidase complex (ABC, 1:300; Vector Laboratories) for 2 h. The sections were then treated with fluorescein isothiocyanate (FITC)-tyramide (1:8,000) and H_2O_2 (0.003%) in Tris hydrochloride buffer (0.05 M, pH = 8.2) for 6 min. The sections were then mounted, dried, and coverslipped in mounting medium.

Microscopy and image processing

Sections were examined using an Olympus BX60 light microscope equipped with fluorescent epi-illumination. Images were captured at 2048 X 2048 pixel resolution with a SPOT Xplorer digital CCD camera (Diagnostic Instruments, Sterling Heights, MI) using a 4-40 X objectives. Confocal images were acquired with a Zeiss LSM 780 confocal Microscope System using 40-63 X objectives at an optical thickness of 1 μm for counting varicosities and 3 μm for counting labeled cell bodies.

For demonstration purposes, contrast and sharpness of the images were adjusted using the ''levels'' and ''sharpness'' commands in Adobe Photoshop CS 9.0. Full resolution of the images was maintained until the final versions were adjusted to a resolution of 300 dpi.

In vitro electrophysiological measurement

Brain slice preparation

Brain slice preparation from adult VGAT-IRES-Cre/Gt (ROSA)26Sor_CAG/ZsGreen1 female mice (n = 3) was carried out as described previously[41] with slight modification. Briefly, after deep isoflurane anesthesia, the animal was decapitated, the brain was removed from the skull and immersed in ice-cold low-Na cutting solution, continuously bubbled with carbogen, a mixture of 95% O_2 and 5% CO_2. The cutting solution contained the following (in mM): saccharose 205, KCl 2.5, $NaHCO_3$ 26, $MgCl_2$ 5, NaH_2PO_4 1.25, $CaCl_2$ 1, glucose 10. Hypothalamic blocks containing the preoptic area were dissected, and 220 μm-thick coronal slices were prepared from the medial preoptic area (MPOA) with a VT-1000S vibratome (Leica Microsystems, Wetzlar, Germany) in the ice-cold low-Na oxygenated cutting solution. The slices were transferred into artificial cerebrospinal fluid (aCSF) (in mM): NaCl 130, KCl 3.5, $NaHCO_3$ 26, $MgSO_4$ 1.2, NaH_2PO_4 1.25, $CaCl_2$ 2.5, glucose 10 bubbled with carbogen and left in it for 1 hour to equilibrate. Equilibration started at 33°C and it was let to cool down to room temperature.

Whole cell patch clamp recording

Recordings were carried out in oxygenated aCSF at 33°C. Axopatch-200B patch-clamp amplifier, Digidata-1322A data acquisition system, and pCLAMP 10.4 software (Molecular Devices, Silicon Valley, CA, USA) were used for recording. VGAT-ZsGreen neurons were visualized with a BX51WI IR-DIC microscope (Olympus, Tokyo, Japan) after identifying them by their fluorescent signal. The patch electrodes (OD = 1.5 mm, thin wall; WPI, Worcester, MA, USA) were pulled with a Flaming-Brown P-97 puller (Sutter

Please cite this article in press as: Keller et al., A thalamo-preoptic pathway promotes social grooming in rodents, Current Biology (2022), https://doi.org/10.1016/j.cub.2022.08.062

Instrument, Novato, CA, USA). The intracellular pipette solution contained (in mM): K-gluconate 130, KCl 10, NaCl 10, HEPES 10, $MgCl_2$ 0.1, EGTA 1, Mg-ATP 4, Na-GTP 0.3. pH = 7.25 with KOH. Osmolarity was adjusted to 300 mOsm with D-sorbitol. Electrode resistance was 2–3 MΩ.

Firing activity of VGAT-ZsGreen neurons was recorded in whole-cell current clamp mode. In order to evoke action potentials even in silent neurons (approx. 30% of the neurons measured) +10 pA holding current was applied during the recordings. Measurements started with a control recording, then PTH2 (8 μM-32 μM, Tocris, UK) was pipetted into the aCSF-filled measurement chamber containing the brain slice in a single bolus and the recording continued. A previously identified selective and potent PTH2 receptor antagonist, HYWH-TIP39[42] was pipetted into the recording chamber just before adding PTH2.

Input resistance and series resistance were monitored at the beginning and at the end of each experiment from the membrane current response to a 20 ms, 5 mV hyperpolarizing voltage step to monitor recording quality. Baseline voltage was also monitored before and after the experiments. All recordings with input resistances (*R*in) < 0.5 GΩ, and series resistances (Rs) > 20 MΩ, or unstable baseline voltage were rejected.

Analysis of patch clamp experiment

Recordings were stored and analyzed off-line. Event detection was performed using the Clampfit module of the PClamp 10.4 software (Molecular Devices, Silicon Valley, CA, USA). Firing rate was calculated as number of action potentials (APs) divided by the length of the corresponding time period (1-1.5-5 min). Area-under-curve values were calculated from these data. Group data were expressed as mean ± standard error of mean (s.e.m). Repeated measures ANOVA was applied to examine whether firing rate change of each group was significant ($p < 0.05$).

QUANTIFICATION AND STATISTICAL ANALYSIS

All statistical tests, significance levels and samples sizes are reported in the figure legends. Sample size *(n)* represents the number of animals per group in each case. All statistical calculations were carried out using GraphPad Prism (GraphPad Software, LLC, released 2020, version 9.0.0.). Data were first tested with Shapiro-Wilk test for normality. If the data were normally distributed, we used two-tailed paired t test for two groups which were related to each other (e. g. social novelty test). When the comparison was made between two different groups, we used two-tailed unpaired t test (e. g. qRT-PCR study or quantification of immunolabeled cells). Otherwise, if the data came from a non-normal distribution, we performed Wilcoxon matched-pairs signed rank test (for comparing two groups) or Friedman test followed by Dunn's multiple comparisons tests (for comparing more groups). In case of the comparison between more than 2 normally distributed groups, two-way ANOVA (e. g. c-Fos quantification) or repeated measures ANOVA (freely moving social behavior test) were performed followed by Šídák's multiple comparisons tests. We list the p value in all cases. Statistical analyses were considered significant for $p < 0.050$ indicated as follows: $0.010 < *p < 0.050$, $0.001 < **p < 0.010$, $***p < 0.001$. All values are expressed as the mean ± s.e.m.

For fiber density analysis of PIL projections and for quantification of the total number of double labeled neurons with c-Fos and PTH2R in the MPOA, we used the machine learning based pixel classification feature of the free bioimage analysis software QuPath v0.2.3 (Queen's University Belfast and University of Edinburg).[33] We determined the area density of the anterogradely labeled nerve fibers (mCherry immunolabeled fiber area/total area) in socially implicated brain regions.